UNIVERSITY OF CALIFORNIA
RIVERSIDE

# Building an Analytical Foundation to Study and Enhance the Bids in Wholesale Electricity Market

A Dissertation submitted in partial satisfaction
of the requirements for the degree of

Doctor of Philosophy

in

Electrical Engineering

by

Mahdi Kohansal

March 2018

Dissertation Committee:

Dr. Hamed Mohsenian-Rad, Chairperson
Dr. Kurt Schwabe
Dr. Salman Asif

The Dissertation of Mahdi Kohansal is approved:

---

---

---

Committee Chairperson

University of California, Riverside

## Acknowledgments

I am grateful to my advisor Dr. Hamed Mohsenian-Rad, whose collective support, guidance, and expertise have made this dissertation a reality. Many thanks to Dr. Kurt Schwabe, Dr. Salman Asif and Dr. Ilya Dumer for their great feedback and being in my thesis committee. Thank you all for sharing your knowledge and passion with me during my Phd program.

I am also thankful of all my lab mates in Smart Grid research Lab. Without their help and support, I couldn't complete my research. I had a wonderful time by working beside you during these four years.

I also extend my gratitude to my family for their unconditional kindness, love, patience, and support throughout my life. They have always been and continue to be my shelter and comfort in this life and especially during my academic career.

And finally, I am really lucky that have awesome friends. They are not only a friend but like a family member to me. They stood beside me in any situations. Thanks to all of you as you make the life easier for me.

This work was supported in part by four NSF grants. The content of this thesis is a reprint of the material that are appeared in the following publications:

- M. Kohansal and H. Mohsenian-Rad, "Sensitivity Analysis of Convergence Bids in Nodal Electricity Markets", accepted for publication in *Proc. of North American Power Symposium*, Morgantown, WV, 2017.

- M. Kohansal, A. Sadeghi-Mobarakeh and H. Mohsenian-Rad, "A Data-driven Analysis of Supply Bids in CAISO Market: Price Elasticity and Impact of Renewables", accepted for publication in *Proc. of the IEEE International Conference on Smart Grid Communications*, Dresden, Germany, October 2017.

- A. Sadeghi-Mobarakeh, M. Kohansal, E. Papalexakis and H. Mohsenian-Rad, "Data Mining based on Random Forest Model to Predict the California ISO Day-ahead Market Prices", in *Proc. of the IEEE Power & Energy Society Conference on Innovative Smart Grid Technologies* (ISGT), Washington, DC, April 2017.

- M. Kohansal and H. Mohsenian-Rad, "A Closer Look at Demand Bids in California Energy Market", in *IEEE Trans. on Power Systems*, Vol. 31, No. 4, pp. 3330-3331, July 2016.

- M. Kohansal and H. Mohsenian-Rad, "Price-Maker Economic Bidding in Two-Settlement Pool-Based Markets: The Case of Time-Shiftable Loads", in *IEEE Trans. on Power Systems*, Vol. 31, No. 1, pp. 695-705, January 2016.

- M. Kohansal and H. Mohsenian-Rad, "Extended-Time Demand Bids: A New Bidding Framework to Accommodate Time-Shiftable Loads", in *Proc. of the IEEE PES General Meeting*, Denver, CO, July 2015.

To my beloved family for all of their patience, kindness, and support.

# ABSTRACT OF THE DISSERTATION

Building an Analytical Foundation to Study and Enhance the Bids
in Wholesale Electricity Market

by

Mahdi Kohansal

Doctor of Philosophy, Graduate Program in Electrical Engineering
University of California, Riverside, March 2018
Dr. Hamed Mohsenian-Rad, Chairperson

An efficient electricity market determines the operational mechanisms to maintain long-term and short-term power system reliability in a least-cost manner. The performance of the market not only depends on the market structure, but also the bidding mechanisms of the market participants including various generation resources, smart consumers and financial players. Our goal is to study and improve the bids in electricity market with focus on the California energy market. Therefore, in this thesis, a comprehensive analysis on the real bidding data from California electricity market has been done. It is concluded that compared to the supply side, the demand side in the California market is currently highly inelastic, leading to many undesirable consequences such as price spikes and exercising market power by generation companies.

To address such issues, a new demand bidding framework has been proposed that recognizes the special characteristics of smart loads. The bids in this framework are called extended-time demand bids. The new framework resolves the problems of accommodating smart loads in the electricity market such as market instability and lack of equilibrium. Moreover, a novel strategy for large smart loads to procure their required energy in electricity market has been introduced. The proposed strategy is general and can be applied to both basic and complex smart load types.

Finally, the performance of financial players bids known as Convergence Bids (CBs) have been studied. While CBs are designed to improve the market efficiency and decrease the price gap between day-ahead and real-time markets, there are recently serious concerns where CBs do not act as intended and their performance even result in decreasing market efficiency. Accordingly, we built an analytical foundation to explain under what conditions placing a CB at a bus in a nodal electricity market can decrease (increase) market efficiency. Specifically, it is shown that transmission line congestion can highly influence the performance of CBs. In particular, under certain transmission line congestion configurations, placing a CB at a bus can result in divergence (instead of convergence) between day-ahead and real-time markets prices.

# Contents

# List of Figures

# List of Tables

# List of Symbols

## Chapter 3

| | |
|---|---|
| $T$ | Number of hours in the hourly market |
| $G$ | Set of supply bids |
| $D$ | Set of demand bids |
| $e$ | Energy component of a bid |
| $p$ | Price component of a bid |
| $\alpha$ | Start-time component of a bid |
| $\beta$ | End-time component of a bid |
| $i$ | Bidder index |
| $t$ | Hourly time index |
| $q$ | Cleared energy in the market |
| $\pi$ | Cleared price in the market |
| $RS$ | Indicating a regular self-schedule bid |
| $RE$ | Indicating a regular economic bid |
| $ES$ | Indicating an extended-time self-schedule bid |
| $EE$ | Indicating an extended-time economic bid |
| $\gamma$ | Penetration of time-shiftable loads |
| $\Delta$ | Time-shiftable load flexible time duration |
| $\lambda, v, \pi$ | Lagrange multipliers in economic dispatch |

## Chapter 4

| | |
|---|---|
| $T$ | number of daily market intervals |
| $t$ | Index of time |
| $k$ | Index of random scenario |
| $l$ | Index of sub-loads |
| $s, n, m, o$ | Indexes of steps in price quota curves |
| $\alpha, \beta$ | Time-shiftable load timing parameters |
| $e$ | Time-shiftable load energy usage parameter |
| $x$ | Energy bid to day-ahead market |
| $y$ | Energy bid to real-time market |
| $p$ | Price bid submitted to the day-ahead market |
| $\lambda$ | Cleared price in day-ahead market |
| $\phi$ | Cleared price in real-time market |
| $q$ | Dispatched energy for economic bid |
| $g$ | Dispatched energy for self-schedule bid |
| $q^{\text{th}}$ | Maximum day-ahead cleared energy at a price |
| $p^{\min}$ | Minimum price at each step of function $q^{\text{th}}$ |
| $a^{\max}$ | Width of each step in function $q^{\text{th}}$ |
| $x^{\min}$ | Minimum energy at each step in function $\lambda$ |
| $b^{\max}$ | Width of each step in function $\lambda$ |
| $y^{\min}$ | Minimum energy at each step in function $\phi$ |
| $c^{max}$ | Width of each step in function $\phi$ |
| $r$ | On and off status of a time-shiftable load |
| $z$ | Total cleared energy in two-settlement markets |
| $Z^{\min}$ | Minimum consumption level |

| | |
|---|---|
| $Z^{\max}$ | Maximum consumption level |
| $D^{\max}$ | Maximum ramp-down rate |
| $U^{\max}$ | Maximum ramp-up rate |
| $\theta, u, v, w$ | Binary auxiliary variables |
| $a, b, c$ | Continuous auxiliary variables |
| $C$ | Energy procurement cost at day-ahead market |

## Chapter 5

| | |
|---|---|
| $\mathbf{x}$, $\mathbf{y}$ | Vectors of physical supply and demand bids at DAM |
| $\mathbf{v}$, $\mathbf{w}$ | Vectors of supply and demand convergence bids |
| $\mathbf{p}$ | Vector of all bids of all types at DAM |
| $\mathbf{z}$ | Vector of physical supply bids at RTM |
| $\boldsymbol{l}$ | Vector of actual demands at time of operation |
| $\boldsymbol{\Phi}$, $\boldsymbol{\Psi}$ | Incidence matrices for $\mathbf{p}$ and $\mathbf{x}$ to system buses at DAM |
| $\boldsymbol{\Theta}$, $\boldsymbol{\Omega}$ | Incidence matrices for $\mathbf{z}$ and $\boldsymbol{l}$ to system buses at RTM |
| $\mathbf{K}$ | Incidence matrix for $\mathbf{p}$ to $\mathbf{x}$ at DAM |
| $\boldsymbol{\pi}$, $\boldsymbol{\mu}$, $\lambda$ | Locational, shadow, and reference prices at DAM |
| $\boldsymbol{\sigma}$, $\boldsymbol{\eta}$, $\delta$ | Locational, shadow, and reference prices at RTM |
| $\bar{\mathbf{D}}$ | Index matrix for congested transmission lines at DAM |
| $\bar{\mathbf{R}}$ | Index matrix for congested transmission lines at RTM |
| $\mathbf{S}$ | Shift factor matrix of the power grid |
| $\mathbf{c}$ | Vector of transmission line capacities |
| $\boldsymbol{\Delta}$ | Vector of price differences: $\boldsymbol{\pi} - \boldsymbol{\sigma}$ |
| $\alpha$, $\beta$ | Coefficients of the cost or utility functions |

# Chapter 1

# Background and Motivation

For decades, and before the electricity market is deregulated, the utility companies used to have monopoly in their service territories. In particular, they used to own the distribution grid, the transmission grid, the majority of the power plants that would generate electricity for their consumers. In some areas, the utilities were run by private companies, while others were public and belonged to city or state governments. Accordingly, the price of electricity was regulated and determined by the city, state, or federal agencies.

In the 1980s, some scholars started arguing that the existing monopoly in the electricity market does not provide incentives to operate efficiency [1, 2]. Furthermore, the lack of competition among utilities and generators has caused unnecessary investment and unwillingness to use new technologies. Based on these arguments, the first power market was created in England and Wales in 1990 [3]. Since then, several power markets have been established around the world, such as in Australia [4] and Spain [5]. In the United States, the electricity markets are mostly regional and operated by Independent System Operators (ISOs). Some of the examples of ISOs that operate deregulated electricity markets include the California ISO (CAISO) [6], the Electric Reliability Council of Texas (ERCOT) [7], and Pennsylvania, Jersey and Maryland (PJM) Interconnect [8].

## 1.1 Electricity Market

**Market Structure:**

After deregulation, the roles of traditional power entities have changed and some new entities have also emerged. These entities can be categorized into four groups:

- Independent System Operators: The ISOs are responsible for running the electricity market, while maintaining the system security. They are called "Independent" because they are non-profit and they are not affiliated with any market participant such as utilities, generators, and end-users. In fact, an ISO should be fair among market participants and provide nondiscriminatory operational service to the market. The priority of ISO is to maintain the system security which includes balancing supply and demand, keeping the frequency of the system in the acceptable range, and removing transmission violations from market transactions. To guarantee maintaining the system security, each ISO has the authority to manage the resources and loads in its service territory. Therefore, besides the role of market operation, the ISO has the responsibility to monitor and control the power grid.

- Generators: They can be of different sizes and types. In practice, it is common that a group of generators belong to the same generation firm. The goal of a generator or a generation firm is to maximize its profit given the opportunities that market may provide. Generators participate in the electricity market by submitting *supply bids*.

- Utilities and Aggregators: A utility or an aggregator is responsible for participating in the market on behalf of consumers. Given the small size of most loads, aggregation is necessary in order to represent loads in the market. Utilities and aggregators participate in the electricity market by submitting *demand bids*.

- Consumers: The electricity consumers are the end users of electricity. While smaller consumers rely on utilities and aggregators to procure electricity, larger consumers,

such as large industrial, agricultural, or commercial users, can directly enter the electricity market and purchase electricity by submitting demand bids.

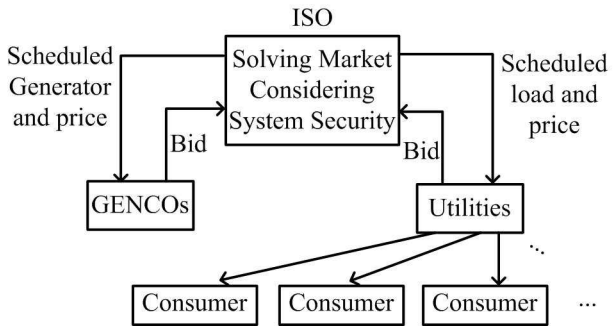


Figure 1.1: Electricity Market Structure

Fig.1.1, shows the relationships among the above entities. The ISO collects the bids and sets the scheduled generation and load as well as the electricity market price.

**Market Price Calculation:**

As we explained earlier, the ISO is responsible for calculating the price of electricity based on the supply and demand bids that it receives. In most existing electricity markets, e.g., in California, supply and demand bids can be either a *self-schedule* bid or an *economic* bid. An economic bid specifies an energy quantity $e$ in MWh and a price quantity $p$ in \$/MWh. If an economic bid is a demand bid it indicates that the buyer is willing to purchase *up to* $e$ MWh energy with a price no higher than $p$ \$/MWh. In contrast, self-schedule bids do not specify any price quantity. For example, a self-schedule demand bid indicates that the buyer is willing to purchase *exactly* $e$ MWh at any cleared market price. In other words, the self-schedule bids represents the price-taker participants in the market, while the economic bids represents the price-maker ones [9–11]. Also, a supply bid is always a *non-decreasing* function of price, while a demand bid is always a *non-increasing* function of price. Examples are shown in Fig. 1.2. First, consider the bid in Fig. 1.2(a). If it

represents a supply bid, then it means that the generator is willing to sell up to 5 MWh of energy, regardless of the price. If the bid in Fig. 1.2(a) represents a demand bid, then it means that the load or utility is willing to buy up to 5 MWh of energy, regardless of the price. Next, consider the bid in Fig. 1.2(b). Since the bid in this figure is a non-decreasing function of price, it may only represent a supply economic bid. It means that the generator is willing to sell up to 4 MWh of energy *only if* the price is 12 $/MWh or higher. Finally, consider the bid in Fig. 1.2(c). Since the bid in this figure is a non-increasing function of price, it may only represent a demand economic bid. It means that the load is willing to buy 6 MWh of energy *only if* the price is 10 $/MWh or less. Moreover, the economic bid may comprise of more than one segment. For instance, CAISO allows the economic bids to be up to 10 segments.

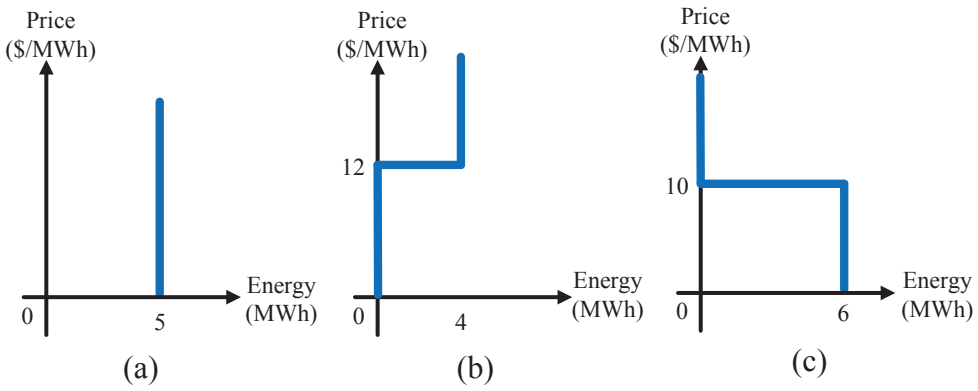


Figure 1.2: Examples for self-schedule and economic bids: (a) A supply or demand self-schedule bid. (b) A supply economic bid. (c) A demand economic bid.

Let $n^{G_{ec}}$ and $n^{L_{ec}}$ denote the number of generators and loads that submit economic bids, respectively. For each generator $i = 1, \ldots, n^{G_{ec}}$, assume that the supply bid is modeled by an energy component $e_i^{G_{ec}} \geq 0$ and a price component $a_i^{G_{ec}} \geq 0$. Similarly, for each load $j = 1, \ldots, n^{L_{ec}}$, assume that the demand bid is modeled by an energy component $e_j^{L_{ec}} \geq 0$ and a price component $b_j^{L_{ec}} \geq 0$. Also, assume that the submitting quantity for self-schedule

bids of supply and load are $e_i^{G_{sf}}$ and $e_i^{L_{sf}}$, respectively. Also, the number of generators and load submitting self-schedule are $n^{G_{sf}}$ and $n^{L_{sf}}$. The ISO clears the market by solving the following optimization problem:

$$
\begin{aligned}
\underset{\boldsymbol{q}^{G_{ec}},\boldsymbol{q}^{L_{ec}}}{\textbf{Maximize}} \quad & \sum_{i=1}^{n^{G_{ec}}} a_i^{G_{ec}} q_i^{G_{ec}} - \sum_{j=1}^{n^{L_{ec}}} b_j^{L_{ec}} q_i^{L_{ec}} \\
\textbf{Subject to} \quad & \sum_{i=1}^{n^{G_{ec}}} q_i^{G_{ec}} + \sum_{i=1}^{n^{G_{sf}}} e_i^{G_{sf}} = \sum_{j=1}^{n^{L_{ec}}} q_i^{L_{ec}} + \sum_{j=1}^{n^{L_{sf}}} e_i^{L_{sf}} \\
& 0 \le q_i^{G_{ec}} \le e_j^{G_{ec}}, \quad i = 1, \ldots, n^{G_{ec}}, \\
& 0 \le q_j^{L} \le e_j^{L_{ec}}, \quad j = 1, \ldots, n^{L_{ec}}.
\end{aligned}
\tag{1.1}
$$

The solution of problem (1.1) directly gives the generation schedule $\boldsymbol{q}^{G_{ec}} = (q_1^{G_{ec}}, \ldots, q_{n^{G_{ec}}}^{G_{ec}})$ and the load schedule $\boldsymbol{q}^{L_{ec}} = (q_1^{L_{ec}}, \ldots, q_{n^{L_{ec}}}^{L_{ec}})$ of the entities that submit economic bids. The cleared market price is also calculated based on the Lagrange multiplier of the equality constraint that shows the power balance between generation and load in the system. The objective in problem (1.1) is to maximize the *social welfare* of all generators and all loads [1].

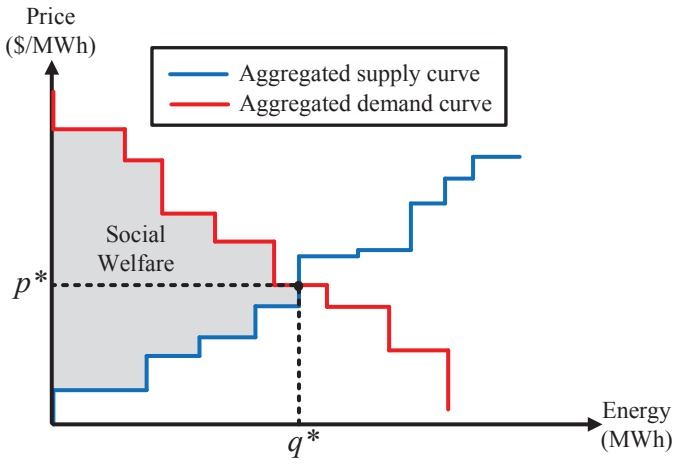


Figure 1.3: The calculation of clearing market price based on supply and demand bids.

The solution of the social welfare maximization problem in (1.1) can also be visualized as in Fig. 1.3. Here, the cleared market price and the generation and load schedules are calculated by crossing the *supply function*, i.e., the aggregation of all supply bids, and the *demand function*, i.e., the aggregation of all demand bids. In this figure, the only economic bids are considered. The shaded area is the optimal social welfare, i.e., the optimal value of the objective function in problem (1.1). Note that, problem in (1.1) does not involve transmission line constraints and the detail of the power transmission network. If we add the transmission line constraints, then the analysis will be generally similar, but more computationally complex. See [1] for more details.

## 1.2 What is the problem?

Traditionally, the focus of feeding the consumers in power systems has been on the generation side. In the recent years, power systems constantly face an increase in the number of electricity consumers. On the other hand, there are limits to what can be achieved on the supply side, because some generating units can take a long time to come up to full power, some units may be very expensive to operate, and demand can at times be greater than the capacity of all the available power plants put together, which can cause the undesirable conditions for market operation. Due to these facts, there is a need to develop new resource management methods to increase the grid efficiency and to better utilize the existing available resources.

Moreover, as shown in chapter 2, since the most of demand entities participate in the market as the price-taker players i.e. by submitting self-schedule bids, they do not influence the market equilibrium price compared to the supply side. Experience with energy markets has shown that the lack of demand participation has been a major contributing factor to occurrences of energy market meltdown. For example, California's energy crisis at the turn of the millennium could, to a large extent, have been mitigated if demand side

would participated in the market by submitting economic bids [12]. Therefore, there is a great need to enhance demand side activity and market participation by encouraging more loads to submit economic bids and also by improving the efficiency of existing demand bids.

## 1.3 Motivation

Given the recent advancements in *smart grid* technologies, such as smart appliances and smart meters, conducting resource management on the demand side has also become a realistic solution to demand side participation in the market. In particular, demand response (DR) programs have recently received great attention in academia and industry [13, 14].

The core idea in DR programs is to exploit load flexibility towards achieving certain energy efficiency or cost reduction goals. In this regard, load flexibility can be defined and modeled in two different ways: load curtailing models and load shifting models. A common model for elastic loads in demand response programs is the load that can be curtailed if needed. In this thesis, we are *not* interested in curtailable loads. Rather we are interested in time-shiftable loads. A time-shiftable load is a task that requires consuming a certain total energy to be completed, but its operation can be scheduled any time before a deadline. Some examples of time-shiftable loads are as follows: charging plug-in electric vehicles [15], irrigation pumps [16], batch processes in data centers and computer servers [17–19], various home appliances such as dish-washer, washing machine, and dryer [20–22], intelligent pools [23], and certain industrial equipment [24, 25].

The operational flexibility in time-shiftable loads makes them a valuable resource in the wholesale electricity market. In fact, they play a central role in creating load flexibility and enhancing demand response and peak-load shaving programs. Also, they can help to enhance demand side market participation by improving the price-responsive behavior of existing demand bids. Therefore, in this thesis, we try to exploit the flexibility of this

type of load to not only minimize the cost of purchasing their energy, but also improve the demand side participation.

Moreover, in the literature, Convergence Bids (CBs) have been considered as a solution to improve the market participation of both the demand and supply sides [26–28]. CBs allow market participants to arbitrage between the forward and spot markets, exempting them from physically consuming or producing energy. The main reason of introducing CBs is to decrease the price gap between forward and spot electricity markets. In fact, in an ideal electricity market, there must be no difference between the prices in these two markets. Recently, several reports from market operators have raised some concerns about the impact of CBs on nodal electricity markets. In particular, there are concerns about cases where CBs do not act as intended and their performance result in decreasing market efficiency even they are increasing market participation. Unfortunately, there is limited literature on addressing the issues related to CBs in electricity markets.

## 1.4 Previous Works

There are a limited number of studies which have looked into real-world bids data in the electricity market [29–32]. Wolfram in [29] studied the bidding behavior of electricity supplies in the daily auction of England and Wales. In [12], the supply and demand bidding during the California market crisis in 2001 have been studied. Also, the authors in [31] and [30] has analyzed the PJM and CAISO market prices and the behavior of supply bids. Also, the elasticity of demand bids in electricity market of Australia and Iran have been studied in [33, 34]. To the best of our knowledge, our analysis in chapter 2 is the first study that addresses the demand bids in CAISO after the market is upgraded to Market Redesign and Technology Upgrade (MRTU) in 2009.

Morever, the operation of time-shiftable loads under demand response paradigm have been discussed in the litreture [35, 36]. Also, recent efforts have been made to incor-

porate *price-taker* time-shiftable loads into the wholesale electricity markets [37–40]. That is, they are assumed to be relatively small so that their operation does *not* have impact on the cleared market price in the day-ahead or real-time markets. For example, the problem of aggregating residential or other time-shiftable loads using utility-driven incentives is discussed in [37, 40, 41]. Moreover, Optimal demand bidding for time-shiftable loads is presented in [42–44], where the time-shiftable load of interest is assumed to be *price-taker*. Furthermore, In [45], an optimal demand bidding mechanism using dynamic programming for time-shiftable loads has been proposed . In this study, both self-scheduling and economic bidding are considered.

The above studies regarding to the accommodating of time-shiftable loads in the electricity market are valid only if the time-shiftable load is small and its operation does *not* affect the price. Given the great interests among utilities to expand their demand response potential, c.f., [46], such price-taker assumption may no longer be accurate in the near future. The wholesale market interaction among *multiple* large time-shiftable loads is investigated in [47] using game theory. It is shown that a market with multiple strategic time-shiftable loads may not always have a Nash equilibrium. That is, such market may not always be stable. In [48, 49], the authors address wholesale electricity market participation of *large* and *price-maker* consumers with time-shiftable and dispatchable loads. However, the focus is on *self-scheduling* operation. That is, the load entity is assumed to submit only energy bids, *but not price bids*. As a result, power procurement is *not* subject to any condition on the clearing market price. Also, the proposed bidding strategy does not improve the demand side participation in the market.

Moreover, the literature on CBs performance in non-electricity markets is rich, c.f. [50–52]. However, the literature on CBs in electricity markets has emerged only recently, and there is limited studies on addressing the issues related to CBs in this market. The common approach so far has been to use historical market data from different ISOs to conduct statistical analysis on market prices. Also, it is yet to be investigated how CBs

may affect the price gap at each market operation time. As for the few studies that take a rather analytical approach to CBs, so far, most of them have focused on cases where the CBs are somewhat abused, either by a market player, e.g., when submitted strategically in conjunction with Financial Transmission Rights (FTR)s [53, 54], or by an adversary, e.g., in a cyber-physical attack [55]. As another example a data-driven approach combined with a game-theoretic analysis was done in [56]. There are a few recent studies that have pointed out the complexities around CBs in electricity markets and the fact that CBs in electricity markets cannot be evaluated in the same way that they are often assessed in other markets [57–59]. However, so far, no prior study has provided any analytical method to explain such complexities and their root causes.

## 1.5 Thesis Organization

This thesis is organized as follow:

**Chapter 2:** We first focus on the real bidding data from the California ISO day-ahead market. Unfortunately, large scale data analysis on real bids data is overlooked in the literature. Therefore, our goal is to make fundamental observations about how demand sides submit bids in the California market as well as the underlying causes and implications of such bidding patterns.

**Chapter 3:** To improve the demand side participation in the market, in section 3, we propose a new demand bidding framework that recognizes the special characteristics of time-shiftable loads. The bids in this bidding framework are called *extended-time demand bids*. The new framework resolves the problems of accommodating time-shiftable loads in the electricity market such as market instability and lack of equilibrium. Moreover, the proposed bidding structure also increases the market competitiveness due to expanding the competition domain and increasing demand elasticity with temporal dependencies.

**Chapter 4:** In this section, a novel strategy for large smart loads to procure their required energy in electricity markets with minimum cost has been introduced. The initial strategy is complex and hard-to-solve optimization problem. A verity of mathematical methods have been applied to transfer the original problem into a tractable linear programming in order to be solved by existing software and computers. As a result, the proposed method becomes practical in the real world and it can be applied by load entities to minimize the cost of procuring their time-shiftable loads in the market.

**Chapter 5:** The Convergence Bids (CBs) have been pointed out as a solution to improve the market participation. More importantly, they help the market to decrease the gap between forward and spot prices. Recently, several reports from ISOs have published that show CBs do not act as intended and their performance result in decreasing market efficiency. Accordingly, in this section, we built an analytical foundation to explain under what conditions placing a CB in a nodal electricity market can decrease (increase) market efficiency.

**Chapter 6:** This chapter concludes this thesis and identifies some future work directions for the research performed in this thesis.

# Chapter 2

# Analysis of Bids in California Electricity Market

## 2.1 Introduction

CAISO operates different types of markets, including a forward market which is known as day-ahead market (DAM). Generators and loads can participate in the CAISO DAM by submitting their bids by 1:00 PM on the day preceding the trading day. In this chapter, and its corresponding paper in [60], our focus is on gaining new insights about market participation and the bids in the CAISO DAM. To the best of our knowledge, our analysis in this section is the first study that addresses the bids; in particular demand bids; in CAISO after the market is upgraded to Market Redesign and Technology Upgrade (MRTU) in 2009.

## 2.2 Basic Observation

In this section, we analyze the bids in CAISO DAM over one year from February 1, 2013 to January 31, 2014. However, our focus is on demand bids since they are not active

player in the market. Two key reports are used from the CAISO Open Access Same-Time Information System [61]. The first report is a detailed database of every self-schedule and economic bid that is submitted to the DAM for each hour on each day. The second report is a summary of the DAM outcome.

In total, we analyzed $365 \times 24 = 8760$ hours of bids. On average, for each hour, CAISO receives supply bids from 523 generators and demand bids from 99 loads. The types and capacities of these bids are shown in Fig. 2.1. From Fig. 2.1(a), although a large number of loads participate in the market, only 7% of them submit economic bids. That means, 93% of loads commit to purchase regardless of the price. In contrast, 44% of generators submit economic bids, as shown in Fig. 2.1(b). As for the size of the bids, only 10% of the total energy demand is elastic, as shown in Fig. 2.1(c). In contrast, 66% of the total energy supply bids are elastic, as shown in Fig. 2.1(d).

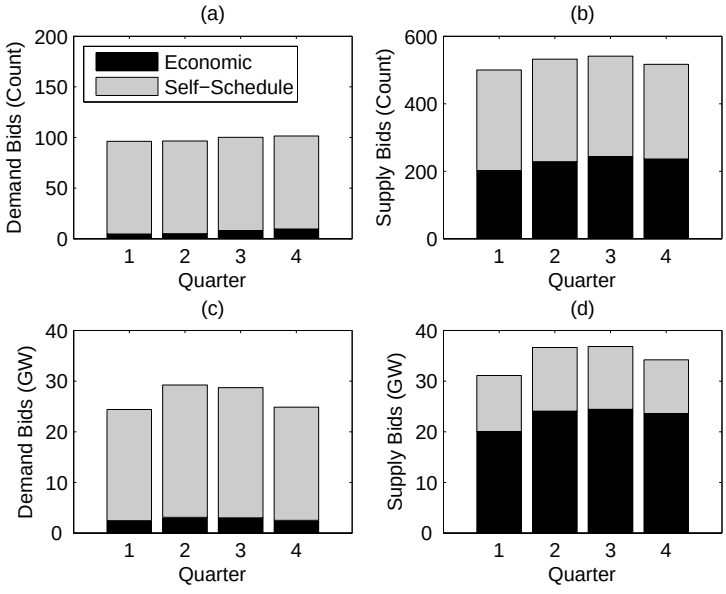


Figure 2.1: The types, counts, and capacities of demand and supply bids across four quarters within the one year duration of this study.

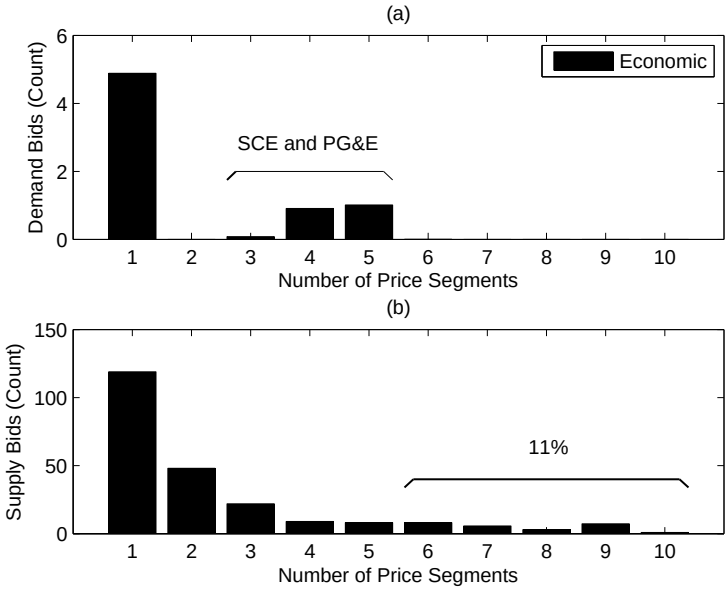


Figure 2.2: The average number of price segments in each economic bid.

A measure to assess the complexity (and to some extent elasticity) of an economic bid is the number of its *price segments*. Even though the economic bids in CAISO market can include up to 10 segments [62] , from Fig. 2.2(a), in practice, most demand bids have only one price segment. It is particularly interesting that *all* economic demand bids that have more than one price segment belong to the two largest utilities in California, namely Southern California Edison (SCE) and Pacific Gas and Electric (PG&E). Surprisingly, the third largest utility in California, i.e., San Diego Gas and Electric (SDG&E) does *not* submit economic bids. It rather submits self-schedule bids and acts as price taker.

On the supply side, the economic bids are much more diverse in terms of the number of their price segments, as shown in Fig. 2.2(b). Interestingly, as high as 11% of generators submit economic bids that include 6 to 10 price segments. This is an important observation specially because we did not see even a single economic demand bid, including the demand bids from SCE and PG&E, with 6 or more price segments.

Next, look at the exact shape of the bids in Figs. 2.3(a) and (b). In both cases, there are four components that form the total demand curve: the bids from the three major utilities and the rest of the bids that are collectively called "Others". Since SDG&E only submits inelastic self-schedule bids, its curves are straight lines. As for Others, they too are practically inelastic bids. Note that, other than about 6 MW load elasticities at $100, which are pointed at by arrows, the rest of the demand curves for Others are straight lines within the practical $0 to $200 price range. Therefore, we can conclude that the price elasticity on the demand side *almost exclusively* comes from the economic bids that are submitted by SCE and PG&E.

For the case in Fig. 2.3(a), which exemplifies a summer day, SCE has a total of 2,976 MW demand elasticity within the price range of $43 to $72; and PG&E has a total of 1,449 MW demand elasticity within the price range of $60 to $150. For the case in Fig. 2.3(b), which exemplifies a winter day, SCE has a total of 1,995 MW demand elasticity within the price range of $54 to $78; and PG&E has a total of 1,146 MW demand elasticity within the price range of $61 to $162. Note that, although the load levels are significantly different in Figs. 2.3(a) and (b), the shapes of bids are similar in the two cases.

Despite their large size of demand elasticity, SCE and PG&E always exploit only 5 or fewer price segments in their bids. The problem with this approach is that it inevitably creates *long sub-ranges of inelastic load*. For example, in Fig. 2.3(a), the SCE demand remains fixed at 14,894 MW even if the price increases by 53% from $45 to $69. As another example, in Fig. 2.3(b), the PG&E demand remains fixed at 9,375 MW even if the price doubles from $70 to $162. Given the fact that SCE and PG&E are the only major loads that currently utilize elastic demand in the CAISO market, these sub-ranges of inelastic load can directly affect the cleared market price and price competitiveness. It is not clear why SCE and PG&E do not exploit all 10 available price segments in their bids.

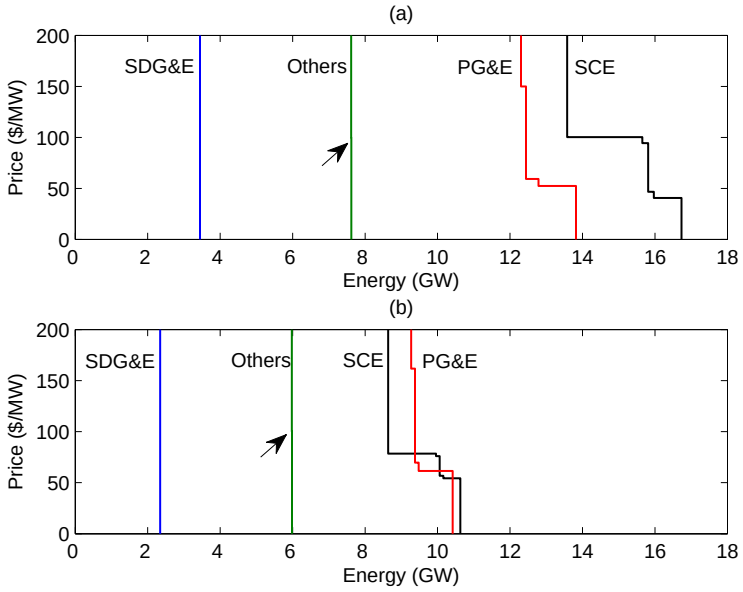


Figure 2.3: Two examples for breaking down the total demand bids across the three major utilities in California. Hours of trading: (a) August 30, 2013 from 4:00 PM to 5:00 PM; (b) January 31, 2014 from 6:00 PM to 7:00 PM.

## 2.3 Further Analysis and Recommendations

### 2.3.1 Implications

From the observations in Section 2, the demand curve in the CAISO day-ahead energy market is, for the most part, a straight line. As a result, the amount of energy that is purchased by loads at each hour in this market does not, for the most part, depend on the cleared market price at that hour. As for the few segments that exist in the aggregate demand curve due to the EBs from SCE and PG&E, while they *do* affect the amount of energy that is purchased from the DAM as a function of the DAM cleared market prices, they do *not* affect the *total* energy that is purchased across the DAM and RTM *combined*. This is due to the fact that the difference between the actual load and the cleared load in the DAM are cleared in the RTM, keeping the *total* demand in the CAISO energy market independent from the cleared market prices. Therefore, *the total demand in the CAISO two-*

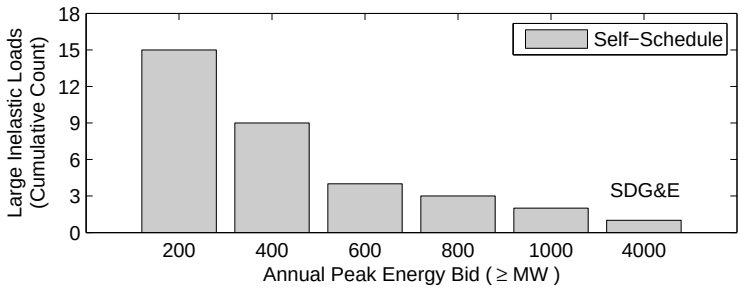


Figure 2.4: The cumulative count of large inelastic loads, with 200 MW or more annual peak energy bids, that do not submit any economic bid at any hour.

*settlement energy market is currently highly inelastic.* Such low elasticity of the demand bids has at least two consequences that are undesirable for efficient operation of the CAISO energy markets: *it may cause price spikes in the DAM and RTM; and it may also facilitate the exercise of market power by generation companies* [63].

### 2.3.2 Underlying Causes

There are at least three reasons for the current demand inelasticity in the CAISO energy market. First, any major and unexpected change in demand due to changes in prices, i.e., any price-elastic load behavior, can have adverse impact on the accuracy of *load forecasting* that is done by CAISO. Since load forecasting plays a central role in CAISO for operating the market and dispatching generation [64], any major deviation of the load from CAISO's forecasted level, due to any reason including price-elasticity, can in turn potentially jeopardize power system reliability or cause unintended price spike.

Second, the primary objective for a load entity when participating in the DAM is to hedge against uncertainty. Specifically, submitting a demand EB is not really about practicing load elasticity and capping the load when the price is high; instead, the intention is often to perform risk management by *diversifying* purchase across DAM and real-time market (RTM). In this sense, the current role of demand EBs is similar to that of another financial tool in CAISO, i.e. convergence bid. Convergence bidding is a mechanism whereby

market participants can make financial purchases (or sales) of energy in the DAM, with the explicit requirement to sell (or buy) back that energy in the RTM; see Chapter 5. Interestingly, while SDG&E does not submit EBs, see Section 2.2, it does submit CBs [65].

Third, there is currently very limited load flexibility available to load entities in California. On one hand, due to various economic and social reasons, the energy usage of many consumers is historically inelastic [63]. On other other hand, the existing load elasticity potential, see Section 2.3.3, has not been utilized yet. For example, the current registered capacity of proxy demand response (PDR) resources is only 37 MW[1].

### 2.3.3 Potentials to Improve Demand Bids

Addressing the three obstacles in Section 2.3.2 can potentially help in enhancing demand bids and increasing load flexibility in the CAISO energy market. First, there is a need to develop new load forecasting methods that incorporate the impact of price-elasticity in demand; see [66]. Load forecasting may also benefit from new demand bidding structures that are designed to accommodate flexible loads; see [67].

Second, we may develop new demand bidding strategies that not only diversify purchase across DAM and RTM, but also exploit various load flexibility potentials to create price-elasticity in demand curves; see [45]. Note that, medium and large consumers are already allowed to directly bid in the CAISO energy markets, where the bids can be as low as 100 kW in total and 10KW in each economic bid segment [64].

Finally, there is a need to make more flexible loads available through enhanced demand response (DR) programs. Some of the current DR programs in CAISO include PDR, reliability demand response resource (RDRR), participating load (PL), and aggregated participating load (APL) [68]. Most of these programs, except for PDR, are mainly designed for ancillary service market participation. However, linking these and other DR programs to energy markets could provide load entities with the *means needed* to practice

[1]This number was provided to the authors by CAISO on March 12, 2015.

price-elasticity. Of course, some load types, such as air conditioners, are minute-scale flexible loads that are best utilized in ancillary service markets. However, there are also load types, such as time-shiftable loads that are hour-scale flexible loads and appropriate for energy market, as long as they are properly aggregated.

## 2.4 Conclusions

We analyzed one year of bids in the CAISO DAM market. We made interesting observations. First, even though about 100 loads participate in the market, the demand curve is shaped by only two loads, SCE and PG&E. This is because almost all other loads submit self-schedule bids with no price components. While, 44% of 523 generators participating in DAM submit economic bid. Second, despite the fact that economic bids can include as many as 10 price segments, the demand bids in California tend to include only 5 or fewer price segments. This has inevitably created long sub-ranges of inelastic load in the demand curve which can potentially affect the cleared market price and price competitiveness. These observations suggest that there is a need for enhancing demand side market participation by encouraging more loads to submit economic bids and also by improving the efficiency of existing economic demand bids.

# Chapter 3

# Extended-Time Demand Bids: A New Bidding Framework to Accommodate Time-Shiftable Loads

## 3.1 Introduction

Recent studies have suggested that time-shiftable loads may face load synchronization and market instability if they are deployed at high penetrations such that they become price maker [47]. To tackle this problem, in this chapter, we propose a new demand bidding framework that recognizes the special characteristics of time-shiftable loads. The new bidding structure is beneficial not only to the power system as a whole but also to the consumers that are capable of shifting a portion of their loads. On one hand, it helps the power system by increasing the social welfare across all generators and loads. On the other hand, time-shiftable loads are cleared at cheaper cost. The new bidding structure

also increases the market competitiveness due to expanding the competition domain and increasing demand elasticity with temporal dependencies. The proposed bidding model incorporates the impact of large and price-maker time-shiftable loads, and it is not prone to load synchronization and market instability.

## 3.2 Bidding Concept and Its Visualization

Consider an electricity market, where an ISO receives and processes the supply and demand bids from generator and load companies, respectively. Currently, the demand bids, whether of type self-schedule or economic, are specific to a particular hour. As a result, they cannot directly accommodate time-shiftable loads. In fact, based on the current market structure, if a demand response aggregator with time-shiftable load seeks to participate in the energy market, then it must submit several separate demand bids at each hour, without having the right tools to indicate the inter-temporal dependency across its bids. As we discussed in Section 3.1, lack of recognizing the time-flexibility in time-shiftable loads can cause market instability [47].

To tackle the above challenges, we propose the concept of extended-time demand bidding as follows:

- *Extended-time Self-Schedule Demand Bid*: It includes an energy quantity $e$, a start-time $\alpha$, and an end-time $\beta$. It indicates that the buyer is willing to purchase an exact total of $e$ MWh at any price and between hours $\alpha$ and $\beta$.

- *Extended-time Economic Demand Bid*: It includes an energy quantity $e$, a price quantity $p$, a start-time $\alpha$, and an end-time $\beta$. It indicates that the buyer is willing to purchase up to a total of $e$ MWh at a price no higher than $p$ \$/MWh between hours $\alpha$ and $\beta$.

Note that, we always have $\alpha \leq \beta$. For the special case where $\alpha = \beta$, an extended-time bid reduces to a regular bid.

Fig. 3.1 shows the impact of time-shiftable self-schedule demand bidding on a two-time-slots market, where $\alpha = 1$ and $\beta = 2$. Once the ISO receives the bid, it must decide on the value of $\theta$, i.e., the portion of the total needed energy $e$ that is going to be procured at hour $\alpha = 1$, while the portion $1 - \theta$ is going to be procured at hour $\beta = 2$. As shown in Figs. 3.1(a) and 3.1(b), by increasing $\theta$, the aggregated demand curve at hour $\alpha = 1$ shifts to the right, resulting in a higher price at this hour, while the aggregated demand curve at hour $\beta = 2$ shifts to the left, resulting in a lower price at this hour. The price curves versus parameter $\theta$ are plotted in Fig. 3.1(c). Considering the two time slots combined, the changes in the total *social welfare* in the power system versus parameter $\theta$ are illustrated in Fig. 3.1(d). Here, the social welfare is calculated across both generators and loads. Based on this curve, the ISO schedules the operation of the time-shiftable load to consume $\theta^* e$ MWh at time slot $\alpha = 1$ and $(1 - \theta^*)e$ at time slot $\beta = 2$. As intended, the total energy consumption adds up to $e$.

## 3.3 Mathematical Representation

In this section, we discuss how the new biding structure can be incorporated into the market optimization problem that is formulated and solved by the ISO. Suppose, the market contains $T = 24$ hours. The economic dispatch problem in presence of extended-time demand bids can be formulated as

$$\begin{aligned} \max_{q} \quad & \sum_{t=1}^{T} \left( \sum_{i \in D_t^{RE}} p_i q_{i,t} - \sum_{j \in G_t^{RE}} p_j q_{j,t} \right) \\ & + \sum_{i \in D_t^{EE}} p_i \left( \sum_{t=\alpha_i}^{\beta_i} q_{i,t} \right) \\ \text{s.t.} \quad & \sum_{i \in D} q_{i,t} = \sum_{j \in G} q_{j,t}, \qquad \forall t \\ & q_{i,t} \leq e_i, \qquad \forall t, \ \forall i \in D^{RE} \end{aligned} \tag{3.1}$$

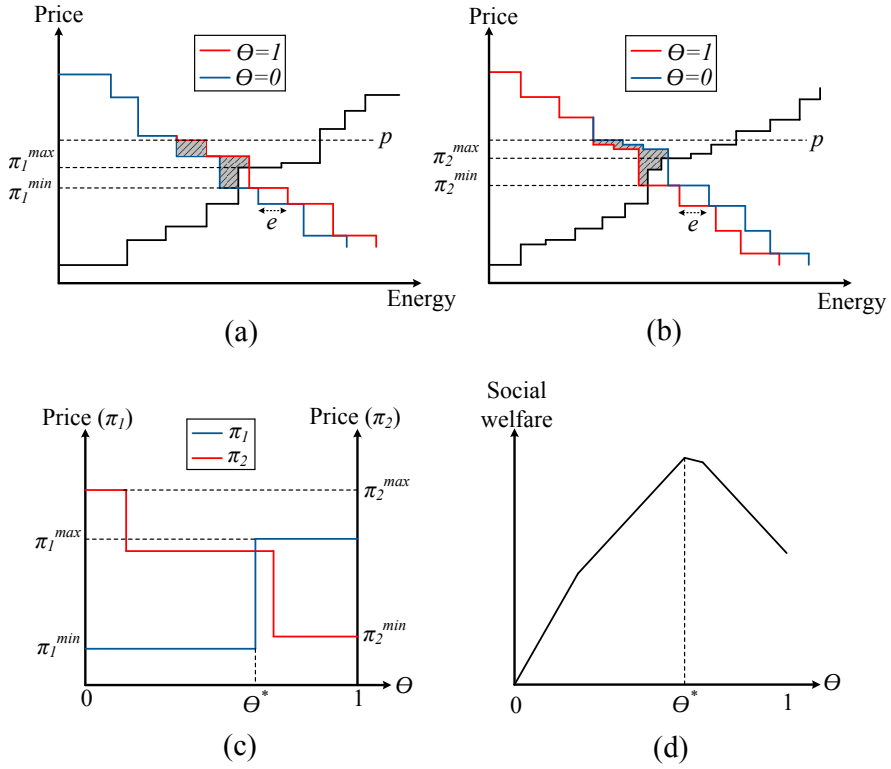


Figure 3.1: Handling an extended-time demand bid in a two-time-slots market: (a) Supply and demand curves at the first hour; (b) Supply and demand curve at the second hour; (c) Price variation with respect to the time-shiftable demand bid at the two hours; (d) Aggregated social welfare across the two hours.

$$
\begin{aligned}
& q_{i,t} = e_i, && \forall t,\ \forall i \in D^{RS} \\
& \sum_{t=\alpha_i}^{\beta_i} q_{i,t} \leq e_i, && \forall i \in D^{EE} \\
& \sum_{t=\alpha_i}^{\beta_i} q_{i,t} = e_i, && \forall i \in D^{ES} \\
& q_{i,t} \geq 0, && \forall t,\ \forall i \in D \\
& \text{Generator } j \text{ Constraints} && \forall j \in G.
\end{aligned}
$$

The objective is to maximize the total social welfare of the power system over the market time horizon. Two changes are made in the economic dispatch problem to incorporate extended-time demand bids. First, in the objective function, the welfare for

each time-shiftable load $i$ that submits extended-time economic demand bid is defined over the entire flexible operation period from $\alpha_i$ to $\beta_i$. Second, in the constraints, the target energy levels for time-shiftable loads are calculated over the entire flexible operation period from $\alpha_i$ to $\beta_i$, whether the extended-time bid is self-schedule or economic.

Next, we derive the Karush-Kuhn-Tucker (KKT) conditions with respect to the extended-time demand bid variables. Suppose $\pi_t$ is the Lagrange multiplier for the energy balance constraint at hour $t$, which represents the price at that hour. Let $\lambda_i$ denote the Lagrange multiplier for total demand constraint for time-shiftable load $i$ and $\upsilon_{i,t}$ denote the Lagrange multiplier for the constraint that shows the cleared energy cannot be negative. The KKT optimality conditions for load $i \in D^{EE}$ and at hour $t$ are obtained as

$$dL/dq_{i,t} = -p_i + \pi_t + \lambda_i - \upsilon_{i,t} = 0, \tag{3.2}$$

$$\lambda_i(\textstyle\sum_{t=\alpha_i}^{\beta_i} q_{i,t} - e_i) = 0, \tag{3.3}$$

$$\lambda_i \geq 0, \tag{3.4}$$

$$\upsilon_{i,t}\ q_{i,t} = 0, \tag{3.5}$$

$$\upsilon_{i,t} \geq 0. \tag{3.6}$$

We can now show the following results:

**Theorem 1**: If the price bid $p_i$ in an extended-time economic demand bid is greater than $\pi_t$, where $\alpha_i \leq t \leq \beta_i$, then the total energy bid $e_i$ will be cleared, i.e., $\sum_{t=\alpha_i}^{\beta_i} q_{i,t} = e_i$

**Proof**: Without loss of generality, let assume that $\pi_{t_0}$ is the minimum price between hour $\alpha_i$ and $\beta_i$. If $p_i > \pi_{t_0}$, then from the KKT conditions, the following relations hold:

$$p_i > \pi_{t_0} \rightarrow p_i - \pi_{t_0} > 0 \rightarrow \lambda_i - \upsilon_{i,t} > 0 \quad ... \tag{3.7}$$
$$... \overset{\upsilon_{i,t} \geq 0}{\longrightarrow} \lambda_i > 0 \rightarrow \sum_{t=\alpha_i}^{\beta_i} q_{i,t} = e_i$$

Similarly, we can show that if $p_i$ is less than the minimum price during hours $\alpha_i$ and $\beta_i$, then the bid is not cleared. ■

From Theorem 1, the behavior of an extended-time economic bid is similar to a regular economic bid, i.e. the cleared energy and the market price match the bidder's desire.

**Theorem 2**: Consider an extended-time bid $i$ and two hours with two different cleared market prices that are within the time frame $\alpha_i$ and $\beta_i$. The amount of cleared energy of this extended-time bid at the more expensive hour is zero.

**Proof**: First, assume that the extended-time bid is of type economic. Suppose $\pi_{t_1} > \pi_{t_2}$, where $t_1$ and $t_2$ are within the time frame $\alpha_i$ and $\beta_i$. Based on the KKT conditions, the following equalities and inequalities hold:

$$\pi_{t_1} > \pi_{t_2} \rightarrow p_i - \lambda_i + \upsilon_{i,t_1} \; > \; p_i - \lambda_i + \upsilon_{i,t_2} \rightarrow ... \tag{3.8}$$
$$... \rightarrow \upsilon_{i,t_1} > \upsilon_{i,t_2} \overset{\upsilon_{i,t_2} \geq 0}{\longrightarrow} \upsilon_{i,t_1} > 0 \rightarrow q_{i,t_1} = 0$$

The case for self-schedule bids can be proved similarly. ■

From the above theorem, the ISO first clears the extended-time bids at the cheapest hours until all prices become equal. After that, the ISO distributes the time-shiftable loads among different hours so that the hourly prices maintain similar.

## 3.4 Benefits of the New Bidding Structure

In this section, we study the impact of applying extended-time demand bids on the California ISO day-ahead energy market. We use the hourly generator and load bids data from the public bids database in [61]. For the ease of presentation, the grid topology and transmission constraints are not considered in our analysis. Moreover, since California ISO does not publish detailed cost of generators such as start-up, ramp up, and ramp down, these parameters are not considered here.

Fig. 3.2 shows the hourly cleared energy and price on January 15, 2014 for different time-shiftable load penetration levels $\gamma$. Here, $\gamma$ % of self-schedule demand bids and $\gamma$ % of economic demand bids are assumed to be replaced by extended-time bids with $\alpha = 1$ and $\beta = 24$. We can see that the amount of cleared load and the cleared market price reduce during peak hours as we increase the penetration of extended-time bids. In fact, the time-shiftable loads have been shifted to off pick hours, causing the peak-to-average ratio (PAR) reduce, which makes the system more reliable. Moreover, by increasing $\gamma$, the prices at different hours become equal, which is predictable based on the Theorem 2. After that, by increasing the penetration level, there will be no change in the market price. Therefore, after a certain penetration threshold, in this case at about $\gamma = 18\%$, the system reaches a saturation point at which increasing $\gamma$ does not affect the cleared market prices.

Fig. 3.3(a) shows the social welfare of the power system versus the penetration of the extended-time bids. We can see that increasing $\gamma$ results in increasing the social welfare. Moreover, as mentioned in section 3.3, besides the system benefits, the extended-time bids are beneficial to the time-shiftable loads. This is shown in Fig. 3.3(b), where the average cleared prices are compared for extended-time and regular demand bids. We can see that the average price of extended-time bids is always less than that of regular bids, especially at lower penetration levels. Based on Theorem 2, in lower amounts of $\gamma$, ISO clears the extended-time bids in off-pick hours which have lower prices. By increasing penetration,

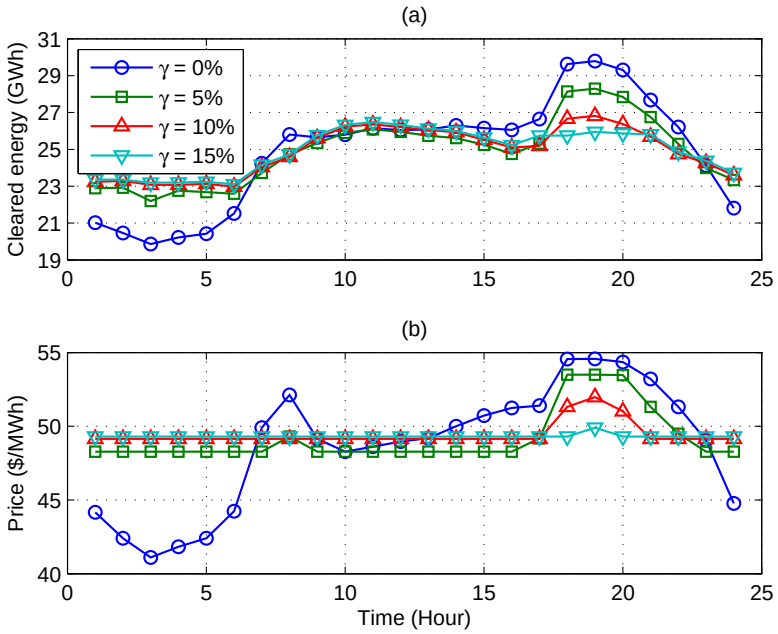


Figure 3.2: Market outcome with extended-time demand bids at different time-shiftable load penetration levels $\gamma$: (a) cleared energy, (b) cleared price.

the system reaches a saturation point, at which the prices become almost equal at different hours. Accordingly, the average prices for different demand bid types converge to each other.

One of the key problems in presentation of time-shiftable loads is *load synchronization*, where all or a large number of time-shiftable loads shift their load to off-peak hours, creating a new peak hour [35,69]. Next, we show that this problem can be tackled if we use extended-time demand bids. The results are shown in Fig. 3.4. Here, the peak-to-average (PAR) is plotted versus the time-shiftable load penetration level for two bidding demand scenarios.

We can see that PAR is high if zero or only a small percentage of the loads are time-shiftable. As we increase $\gamma$, the PAR reduces almost similarly for the two demand bidding scenarios. However, beyond a certain penetration level when there is a considerable percentage of time-shiftable loads, the PAR starts increasing, instead of decreasing, if the

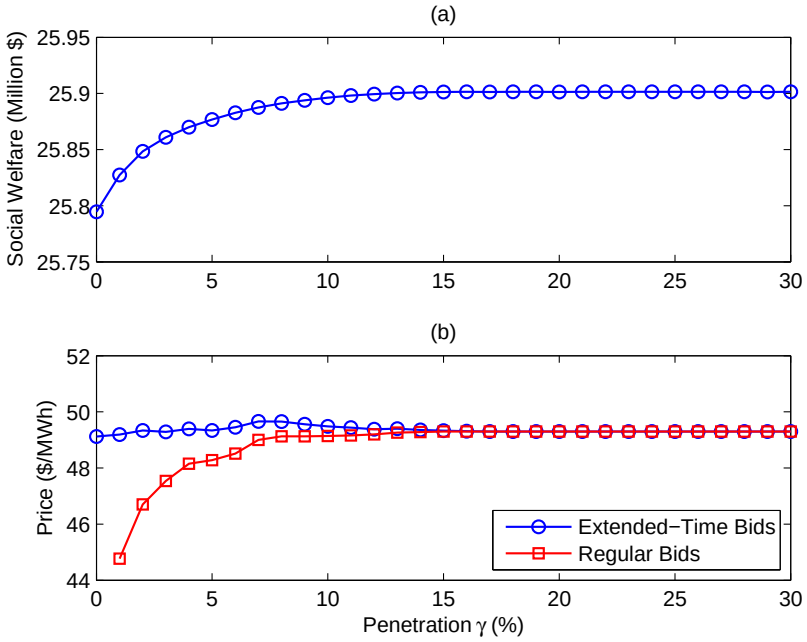


Figure 3.3: Market parameters versus the penetration of extended-time bids: (a) Social welfare, (b) Average market price for different types of demand bids.

regular demand bids are used for time-shiftable loads. This is due to the load synchronization problem that we mentioned earlier. However, by applying the proposed extended-time bidding framework, we continue benefiting from the time-flexibility in time-shiftable loads and lowering the prices even at higher penetrations of time-shiftable loads without suffering from load synchronization.

Finally, we assess the market outcome for different values of $\Delta = \beta - \alpha + 1$, i.e., the flexible time duration for time-shiftable loads. The results are shown in Fig. 3.5. We can see that increasing $\Delta$ can potentially help in peak load shaving and lower peak load prices. However, by comparing the results in Figs. 3.2 and 3.5, one can conclude that increasing the penetration of time-shiftable loads, i.e., the volume of flexible loads is often more beneficial compared to increasing the time flexibility of a small volume of time-shiftable loads.

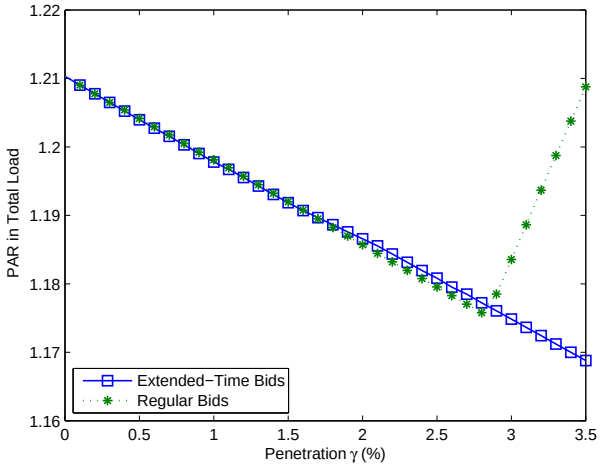


Figure 3.4: The peak-to-average ratio of the total load profit versus the penetration level of the time-shiftable loads. The load synchronization problem is resolved.

## 3.5 Impact on Market competitiveness

In this section, we present an example to study the impact of extended-time demand bidding on price competitiveness. Consider a market over $T = 3$ hours. The true generation and demand bids based on the true marginal costs are shown in Tables 3.1 and 3.2, respectively. Since self-schedule bidding is a special case of economic bidding, where the price bid is infinity, all bids are assumed to be economic bids. There are 11 generators and 11 loads in each time slot. Let us assume that generator $j = 3$ at hour $t = 1$, generator $j = 5$ at hour $t = 2$ and generator $j = 4$ at hour $t = 3$ submit their bids strategically. Similar to the previous section, we assumed that a portion $\gamma$ of each load is time-shiftable, where $\alpha = 1$ and $\beta = 3$. To find Nash equilibrium among the three strategically bidding generators, we followed the general method in [70] and used an exhaustive search with resolution 1\$/MWh for the price bid and 1MWh for energy bid. The results are shown in Table 3.3. We can see that by increasing $\gamma$, the differences between noncompetitive and competitive prices reduces. It means that by applying extended-time bids, there is less potential for the three strategic generators to exercise market power. Furthermore, at $\gamma = 16\%$, one

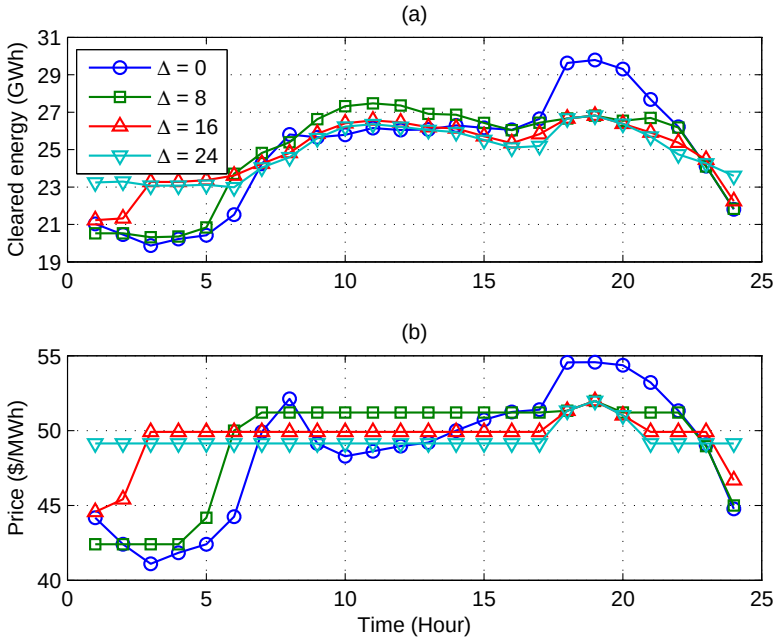


Figure 3.5: Market outcome with extended-time demand bids at different time-shiftable load durations $\Delta$: (a) cleared energy, (b) cleared price.

of the Nash equilibria under extended-time bidding is equal to the true market equilibrium and the prices at the other equilibrium point are only 1$ more than the competitive prices. In contrast, at $\gamma = 0$, which is the representation of the existing market framework, the differences of the cleared and competitive prices are $32-28 = \$4$ at hour $t = 1$, $36-30 = \$6$ at hour $t = 2$, and $38 - 35 = \$3$ at hour at $t = 3$.

## 3.6 Conclusion

In this chapter, we propose extended-time demand bids that are tailored around the special characteristics of time-shiftable loads. The proposed new bidding framework is compatible with the existing market structures as it allows both self-schedule and economic bids to become extended-time demand bids. The bidding concept, its visualization, and its

Table 3.1: Generators bids data

| Generator Index $j$ | (Energy $e$, Price $p$) | | |
|---|---|---|---|
| | $t = 1$ | $t = 2$ | $t = 3$ |
| 1 | (10 , 5) | (14 , 4) | (10 , 2) |
| 2 | (8 , 7) | (11 , 9) | (7 , 7) |
| 3 | (25 , 11) | (12 , 16) | (12 , 14) |
| 4 | (15 , 17) | (10 , 21) | (20 , 27) |
| 5 | (14 , 25) | (30 , 28) | (10 , 23) |
| 6 | (10 , 28) | (10 , 33) | (11 , 30) |
| 7 | (12 , 40) | (6 , 41) | (6 , 35) |
| 8 | (10 , 48) | (13 , 45) | (13 , 40) |
| 9 | (10 , 55) | (9 , 49) | (9 , 44) |
| 10 | (11 , 60) | (11 , 53) | (11 , 51) |
| 11 | (9 , 68) | (15 , 59) | (15 , 57) |

mathematical representation are presented. It is shown that the proposed bidding structure can prevent the typical load synchronization problem for time-shiftable loads. Furthermore, it is beneficial to the power system as a whole and the consumers with time-shiftable loads. The new demand bidding structure also has the potential to increase the market competitiveness and contribute to mitigating market power.

Table 3.2: Demand bids data

| Load Index $i$ | (Energy $e$, Price $p$) | | |
|---|---|---|---|
| | $t = 1$ | $t = 2$ | $t = 3$ |
| 1 | (23 , 84) | (14 , 85) | (10 , 80) |
| 2 | (12 , 72) | (17 , 74) | (10 , 72) |
| 3 | (17 , 59) | (15 , 65) | (15 , 62) |
| 4 | (10 , 51) | (9 , 54) | (12 , 53) |
| 5 | (9 , 44) | (11 , 48) | (10 , 46) |
| 6 | (9 , 32) | (10 , 36) | (7 , 40) |
| 7 | (10 , 27) | (9 , 30) | (8 , 38) |
| 8 | (12 , 23) | (10 , 26) | (7 , 32) |
| 9 | (14 , 13) | (11 , 18) | (11 , 27) |
| 10 | (10 , 8) | (13 , 10) | (12 , 20) |
| 11 | (7 , 5) | (7 , 6) | (14 , 11) |

Table 3.3: Market Price Competitiveness

| Penetration $\gamma$ | Noncompetitive Price ($) | | | Competitive Price ($) | | |
|---|---|---|---|---|---|---|
| | $t = 1$ | $t = 2$ | $t = 3$ | $t = 1$ | $t = 2$ | $t = 3$ |
| 0% | 32 | 36 | 38 | 28 | 30 | 35 |
| 8% | 33 | 33 | 35 | 32 | 32 | 32 |
| | 32 | 32 | 35 | | | |
| 16% | 33 | 33 | 33 | 32 | 32 | 32 |
| | 32 | 32 | 32 | | | |

# Chapter 4

# Price-Maker Economic Bidding in Two-Settlement Pool-Based Markets: The Case of Time-Shiftable Load

## 4.1 Introduction

In this section, a new scenario-based stochastic optimization framework is proposed for price-maker economic bidding in day-ahead market (DAM) and real-time market (RTM) [11, 71]. The presented methodology is general and can be applied to both demand and supply bids. That is, no restrictive assumptions are made on the characteristics of the pool and its agents. However, our focus is on the operation of time-shiftable loads with deadlines, because; as mentioned in Chapter 1; they play a central role in creating load flexibility and demand side participation. Moreover, we *do* consider the size of the load and hence the impact of demand bids on the cleared market price. In fact, the analysis in

this section advances the existing *price-taker* results in [45], because here we consider *price-maker* market participation of time-shiftable loads. This study also advances the existing *self-scheduling* results in [72], because here we consider *economic* bidding. In our model, we consider *two-settlement* markets, where energy is procured from both DAM and RTM. Note that, the electricity markets in the united states have been designed based on the two-settlements; therefore, the result of this section is applicable in real world electricity markets.

## 4.2 Problem Statement

### 4.2.1 Two-Settlement Electricity Market

In a two-settlement wholesale electricity market, e.g., in California , Pennsylvania-Jersey-Maryland, and Texas, energy is traded in both DAM and RTM. Also from chapter 1 , there are more energy cost minimization opportunities for loads in Economic bidding than Self-Schedule bidding. However, the demand bids that are submitted (or metered) to the real-time market only indicate energy quantities. That is, they are always of type Self-Schedule [44, 73].

**Day-Ahead Market:**

Let $T$ denote the number of daily market intervals. For example, in an hourly market, we have $T = 24$. At each time slot $t$, let $x_t$ and $p_t$ denote the energy bid and the price bid that are submitted to the day-ahead market, respectively. The market outcome from a participant perspective depends on not only its bids, but also the market *price quota curve*[1] [72], [74], as shown in Fig. 4.1. There are one self-schedule and two economic bids

[1] "For a given hour, the *quota* of a price maker generator or load is defined as the amount of power that it generates or consumes in that hour. The curve that expresses how the market-clearing price changes as this quota changes is called residual generation/demand curve [74] or simply price quota curve [72]. While the price quota curve is *step-wise monotonically decreasing* with respect to generation level for a price maker generator, it is *step-wise monotonically increasing* with respect to consumption level for a price maker

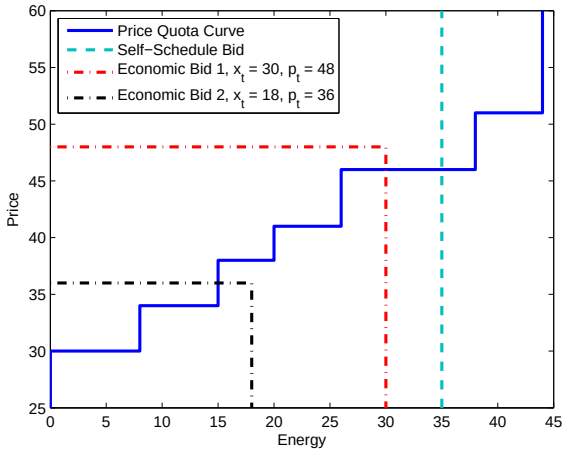


Figure 4.1: An example for price-maker self-scheduling and price-maker economic bidding for a given price quota curve in a pool-based market.

shown in this figure. The self-schedule bid is a straight vertical line. Moving this line towards left or right can affect the price, as explained in the price-maker self-scheduling analysis in [72]. In contrast, price-maker economic bids affect not only the price but also the amount of cleared energy quantity, as shown in Figs. 4.2(a) and (b), respectively. In fact, under price-maker economic bidding, the cleared market price and the cleared energy quantity are *two-dimensional* functions $\lambda_t(x_t, p_t)$ and $q_t(x_t, p_t)$, respectively. For each price bid $p_t$, the cleared market price $\lambda_t(x_t, p_t)$ is a step-wise increasing function of energy bid $x_t$. Also, for each price bid $p_t$, the cleared energy quantity $q_t(x_t, p_t)$ is a straight identity line that is *saturated* beyond a certain threshold. Such threshold increases as the price bid $p_t$ increases, allowing larger energy bids to be cleared in the day-ahead market. For the example in Fig. 4.2, if the energy bid is $x_t = 20$ MW and the price bid is $p_t = 36$ \$/MW, then we have $\lambda_t(x_t, p_t) = 36$ \$/MW and $q_t(x_t, p_t) = 15$ MW. If $x_t = 20$ MW and $p_t = 48$ \$/MW, then we have $\lambda_t(x_t, p_t) = 38$ \$/MW and $q_t(x_t, p_t) = 20$ MW. These numbers are marked on Fig. 4.2 for clarification.

consumer. Price quota curves are stepwise because the supply/demand bids are assumed to be blocks of generation/load at given prices [72]. These curves embody the effects of all interactions with competitors and the market rules [72], [74]. The price quota curves of a price maker generator or load can be obtained

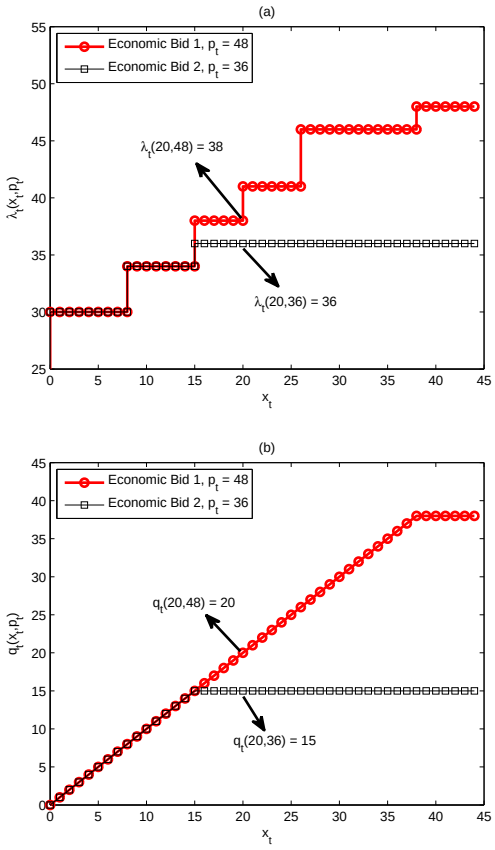


Figure 4.2: An example for the market outcome under price-maker economic bidding for two different price bids: (a) cleared price of electricity; (b) cleared energy quantity. Here, the price quota curve is the same as the one in Fig. 1.

**Real-Time Market:**

Recall from Section 2 that the demand bids in real-time markets do not indicate any price quantity. In fact, in practice, the demand is only metered and then the payments corresponding to the real-time markets are calculated accordingly [76]. At each time slot $t$, let $y_t$ denote the energy bid that is submitted (or metered) to the real-time market. The cleared market price and the cleared energy quantity are modeled as *one-dimensional* functions $\phi_t(y_t)$ and $g_t(y_t)$, respectively. The former is a step-wise increasing function of energy bid $y_t$. The latter is simply a straight identity line, i.e., $g_t(y_t) = y_t$.

by either market simulation or using forecasting procedures [74], [75].

### 4.2.2 Optimization Problem

In practice, market participation is prone to *uncertainty*. Let $K$ denote the number of random market scenarios. At each time slot $t$ and for each scenario $k = 1, \ldots, K$, the multiplications $q_{t,k}(x_t, p_t)\lambda_{t,k}(x_t, p_t)$ and $y_{t,k}\phi_{t,k}(y_{t,k})$ indicate the cost of power procurement from the day-ahead market and the real-time market, respectively. The price-maker economic bidding problem for time-shiftable loads can be formulated as

$$\begin{aligned} \textbf{min} \quad & \frac{1}{K}\sum_{k=1}^{K}\sum_{t=\alpha}^{\beta} q_{t,k}(x_t, p_t)\lambda_{t,k}(x_t, p_t) + y_{t,k}\phi_{t,k}(y_{t,k}) \\ \textbf{s.t.} \quad & \sum_{t=\alpha}^{\beta} q_{t,k}(x_t, p_t) + y_{t,k} = e, \qquad \forall\, k, \end{aligned} \tag{4.1}$$

where the optimization variables are $x_t$, $p_t$, and $y_{t,k}$ for any time slot $t$ and any market scenario $k$. The objective in (4.1) is to minimize the expected value of the total energy expenditure to finish the task. The equality constraints assure that for all scenarios, the total energy purchased matches the target energy level $e$. Note that, the energy bids to real-time market act as *resource variables* [77, 78]. As a result, they are specific to each scenario $k$ to purchase a total of $e - \sum_{t=\alpha}^{\beta} q_{t,k}(x_t, p_t)$ MWh energy from the real-time market under scenario $k$.

The nonlinear mixed-integer stochastic optimization problem in (4.1) is difficult to solve. In fact, it is recently shown in [45] that even if the time-shiftable load is small and price-taker, i.e., $\lambda_{t,k}$ and $\phi_{t,k}$ are independent of the bids, then solving problem (4.1) is still a challenging task due to the nonlinearity in $q_{t,k}(x_t, p_t)$. Nevertheless, we will next present an innovative method to find the global optimal solution of problem (4.1) within a short amount of computational time.

## 4.3 Proposed Solution Method

In this section, we explain how we can reformulate problem (4.1) as a mixed-integer linear program. This is done by taking four key steps. The reformulated optimization problem is then solved efficiently using various mixed-integer linear programming solvers, such as CPLEX [79] or MOSEK [80].

### 4.3.1 Problem Reformulation Steps

**Step 1**: At each time slot $t$ and for each scenario $k$, we define $q^{\text{th}}_{t,k}(p_t)$ as the maximum energy quantity that can be cleared in the day-ahead market when the price bid is $p_t$. For example, from Fig. 2(b), we have $q^{\text{th}}_{t,k}(36) = 15$ MWh. This is because the cleared energy curve for any bid with $p_t = \$36$ is bounded by 15 MWh. In other words, if the time-shiftable load seeks to procure more than 15 MWh, then it must submit a price bid that is higher than \$36. As another example, we have $q^{\text{th}}_{t,k}(48) = 38$ MWh. A method to model $q^{\text{th}}_{t,k}(p_t)$ will be provided later in Step 3. However, for now, assume that the value of $q^{\text{th}}_{t,k}(p_t)$ is given for each price bid $p_t$. We can write

$$q_{t,k}(x_t, p_t) = \begin{cases} x_t, & \text{if } x_t \leq q^{\text{th}}_{t,k}(p_t), \\ q^{\text{th}}_{t,k}(p_t), & \text{otherwise.} \end{cases} \tag{4.2}$$

In other words, we have

$$q_{t,k}(x_t, p_t) = \min\Big\{x_t,\ q^{\text{th}}_{t,k}(p_t)\Big\}. \tag{4.3}$$

Next, we define a new auxiliary variable as

$$\theta_{t,k} = \begin{cases} 0, & \text{if } x_t \leq q^{\text{th}}_{t,k}(p_t), \\ 1, & \text{otherwise.} \end{cases} \tag{4.4}$$

From (4.2), (4.3) and (4.4), we have

$$\theta_{t,k} = 0 \quad \Leftrightarrow \quad q_{t,k}(x_t, p_t) = x_t \leq q^{\text{th}}_{t,k}(p_t) \tag{4.5}$$

and

$$\theta_{t,k} = 1 \quad \Leftrightarrow \quad q_{t,k}(x_t, p_t) = q^{\text{th}}_{t,k}(p_t) \leq x_t. \tag{4.6}$$

Interestingly, for any time slot $t$ and any market scenario $k$, the relationships in (4.5) and (4.6) are equivalent to

$$\theta_{t,k} \in \{0, 1\}, \tag{4.7}$$

$$x_t - \theta_{t,k} L \leq q_{t,k}(x_t, p_t) \leq x_t, \tag{4.8}$$

$$q^{\text{th}}_{t,k}(p_t) - (1 - \theta_{t,k})L \leq q_{t,k}(x_t, p_t) \leq q^{\text{th}}_{t,k}(p_t), \tag{4.9}$$

where $L$ is a large number compared to load size $e$. To show the above, we note that, if $\theta_{t,k} = 0$, then (4.8) and (4.9) become

$$x_t \leq q_{t,k}(x_t, p_t) \leq x_t, \tag{4.10}$$

$$q^{\text{th}}_{t,k}(p_t) - L \leq q_{t,k}(x_t, p_t) \leq q^{\text{th}}_{t,k}(p_t). \tag{4.11}$$

The lower bound and the upper bound in (4.10) are equal. Also, since $L$ is a large number, the lower bound constraint in (4.11) is not binding. Therefore, we can conclude that the relationship in (4.5) holds. If $\theta_{t,k} = 1$, then (4.8) and (4.9) become

$$x_t - L \leq q_{t,k}(x_t, p_t) \leq x_t, \tag{4.12}$$

$$q^{\text{th}}_{t,k}(p_t) \leq q_{t,k}(x_t, p_t) \leq q^{\text{th}}_{t,k}(p_t), \tag{4.13}$$

The lower bound constraint in (4.11) is not binding. From this and because the lower bound

and the upper bound in (4.10) are equal, we can conclude the relationship in (4.6).

**Step 2**: At each time slot $t$ and for each scenario $k$, the cleared market price in the day-ahead market is obtained as

$$\lambda_{t,k}(x_t, p_t) = \begin{cases} \lambda_{t,k}(x_t, \infty) & \text{if } x_t \leq q^{\text{th}}_{t,k}, \\ p_t & \text{otherwise,} \end{cases} \tag{4.14}$$

where $\lambda_{t,k}(x_t, \infty)$ is the price quota curve for an infinite price bid, i.e., the price curve under Self-Scheduling [72]. Next, we note that the cost of power procurement from the day-ahead market at time slot $t$ and under scenario $k$ is modeled as

$$C_{t,k}(x_t, p_t) = q_{t,k}(x_t, p_t)\, \lambda_{t,k}(x_t, p_t). \tag{4.15}$$

From (4.2) and (4.14), we can rewrite the above expression as

$$C_{t,k}(x_t, p_t) = \begin{cases} x_t \lambda_{t,k}(x_t, \infty) & \text{if } x_t \leq q^{\text{th}}_{t,k}, \\ q^{\text{th}}_{t,k}(p_t) p_t & \text{otherwise.} \end{cases} \tag{4.16}$$

If $x_t \leq q^{\text{th}}_{t,k}(p_t)$ then $\lambda_{t,k}(x_t, \infty) \leq p_t$. Accordingly, we have $x_t \lambda_{t,k}(x_t, \infty) \leq q^{\text{th}}_t(p_t) p_t$. Also, if $x_t > q^{\text{th}}_t(p_t)$ then $\lambda_{t,k}(x_t, \infty) \geq p_t$. Accordingly, we have $x_t \lambda_{t,k}(x_t, \infty) \geq q^{\text{th}}_t(p_t) p_t$. Therefore, we can rewrite (4.16) as

$$C_{t,k}(x_t, p_t) = \min \Big\{ x_t \lambda_{t,k}(x_t, \infty),\ q^{\text{th}}_{t,k}(p_t) p_t \Big\}. \tag{4.17}$$

From (4.4), (4.16) and (4.17), we have

$$\theta_{t,k} = 0 \ \Leftrightarrow\ C_{t,k}(x_t, p_t) = x_t \lambda_{t,k}(x_t, \infty) \leq q^{\text{th}}_{t,k}(p_t) p_t \tag{4.18}$$

and

$$\theta_{t,k} = 1 \;\Leftrightarrow\; C_{t,k}(x_t, p_t) = q^{\text{th}}_{t,k}(p_t)p_t \leq x_t\lambda_{t,k}(x_t, \infty). \tag{4.19}$$

Again, for any time slot $t$ and any market scenario $k$, the relationships in (4.18) and (4.19) are equivalent to (4.7) and

$$x_t\lambda_{t,k}(x_t, \infty) - \theta_{t,k}L \leq C_{t,k}(x_t, p_t) \leq x_t\lambda_{t,k}(x_t, \infty), \tag{4.20}$$

$$q^{\text{th}}_t(p_t)p_t - (1 - \theta_{t,k})L \leq C_{t,k}(x_t, p_t) \leq q^{\text{th}}_t(p_t)p_t, \tag{4.21}$$

where $L$ is again a large number. To show the above equivalence, we note that if $\theta_{t,k} = 0$, then (4.20) and (4.21) become

$$x_t\lambda_{t,k}(x_t, \infty) \leq C_{t,k}(x_t, p_t) \leq x_t\lambda_{t,k}(x_t, \infty), \tag{4.22}$$

$$q^{\text{th}}_t(p_t)p_t - L \leq C_{t,k}(x_t, p_t) \leq q^{\text{th}}_t(p_t)p_t. \tag{4.23}$$

The lower bound and the upper bound in (4.22) are equal. Also, since $L$ is a large number, the lower bound constraint in (4.23) is not binding. Therefore, we can conclude that the relationship in (4.18) holds. If $\theta_{t,k} = 1$, then (4.20) and (4.21) become

$$x_t\lambda_{t,k}(x_t, \infty) - L \leq C_{t,k}(x_t, p_t) \leq x_t\lambda_{t,k}(x_t, \infty), \tag{4.24}$$

$$q^{\text{th}}_t(p_t)p_t \leq C_{t,k}(x_t, p_t) \leq q^{\text{th}}_t(p_t)p_t. \tag{4.25}$$

The lower bound constraint in (4.24) is not binding. From this and because the lower bound and the upper bound in (4.25) are equal, we can conclude the relationship in (4.19).

**Step 3**: At each time slot $t$ and for each scenario $k$, the threshold $q^{\text{th}}_{t,k}(p_t)$ is a step-wise linear function of price bid $p_t$. For example, in Fig. 1, $q^{\text{th}}_{t,k}(p_t)$ is 0 for any $p_t < 30$, it is 8 for any $30 \leq p_t < 34$, it is 15 for any $34 \leq p_t < 38$, and so on and so forth. Following

the general methodology in [72] for modeling step-wise linear functions, we can write

$$q_{t,k}^{\text{th}}(p_t) = \sum_{i=1}^{n_{t,k}} x_{t,k,s}^{\min} u_{t,k,s}, \tag{4.26}$$

$$p_t = \sum_{i=1}^{n_{t,k}} \left(a_{t,k,s} + u_{t,k,s} p_{t,k,s}^{\min}\right), \tag{4.27}$$

where

$$u_{t,k,s} \in \{0,1\}, \tag{4.28}$$

$$0 \leq a_{t,k,s} \leq u_{t,k,s} a_{t,k,s}^{\max}, \tag{4.29}$$

$$\sum_{s=1}^{n_{t,k}} u_{t,k,s} = 1. \tag{4.30}$$

Here, $n_{t,k}$ is the number of price steps in the step-wise linear function $q_{t,k}^{\text{th}}(p_t)$, parameter $p_{t,k,s}^{\min}$ is the minimum price in step number $s$, parameter $x_{t,k,s}^{\min}$ is the cleared energy in step number $s$, parameter $a_{t,k,s}^{\max}$ is the width of step number $s$, $v_{t,k,s}$ and $a_{t,k,s}$ are auxiliary variables. For example, in Fig. 1, we have $p_{t,k,1}^{\min} = 0$, $p_{t,k,2}^{\min} = 30$, $p_{t,k,3}^{\min} = 34$, $p_{t,k,4}^{\min} = 38$, $x_{t,k,1}^{\min} = 0$, $x_{t,k,2}^{\min} = 8$, $x_{t,k,3}^{\min} = 15$, $x_{t,k,4}^{\min} = 20$, $a_{t,k,1}^{\max} = 30$, $a_{t,k,2}^{\max} = 4$, $a_{t,k,3}^{\max} = 4$, $a_{t,k,4}^{\max} = 3$, etc. We can also write

$$q_{t,k}^{\text{th}}(p_t)\, p_t = \sum_{s=1}^{n_{t,k}} x_{t,k,s}^{\min} \left(c_{t,k,s} + v_{t,k,s} p_{t,k,s}^{\min}\right). \tag{4.31}$$

**Step 4**: Finally, at each time slot $t$ and for each scenario $k$, we can again adjust the modeling approach in [72] and write:

$$x_t \lambda_{t,k}(x_t, \infty) = \sum_{s=1}^{m_{t,k}} \lambda_{t,k,s} \left(b_{t,k,s} + v_{t,k,s} x_{t,k,s}^{\min}\right), \tag{4.32}$$

$$x_t = \sum_{s=1}^{m_{t,k}} \left(b_{t,k,s} + v_{t,k,s} x_{t,k,s}^{\min}\right), \tag{4.33}$$

and

$$y_{t,k}\phi_{t,k}(y_{t,k}) = \sum_{s=1}^{o_{t,k}} \phi_{t,k,s}\left(c_{t,k,s} + w_{t,k,s}y_{t,k,s}^{\min}\right), \tag{4.34}$$

$$y_{t,k} = \sum_{s=1}^{o_{t,k}} \left(c_{t,k,s} + w_{t,k,s}y_{t,k,s}^{\min}\right), \tag{4.35}$$

where

$$v_{t,k,s} \in \{0,1\}, \tag{4.36}$$

$$w_{t,k,s} \in \{0,1\}, \tag{4.37}$$

$$0 \le b_{t,k,s} \le v_{t,k,s}b_{t,k,s}^{\max}, \tag{4.38}$$

$$0 \le c_{t,k,s} \le w_{t,k,s}c_{t,k,s}^{\max}, \tag{4.39}$$

$$\sum_{s=1}^{m_{t,k}} v_{t,k,s} = 1, \tag{4.40}$$

$$\sum_{s=1}^{o_{t,k}} w_{t,k,s} = 1. \tag{4.41}$$

Here, parameters $m_{t,k}$, $x_{t,k,s}^{\min}$, and $b_{t,k,s}^{\max}$ characterize the step-wise linear day-ahead price quota curve $\lambda_{t,k}(x_t, \infty)$ under Self-Schedule bidding; and $o_{t,k}$, $y_{t,k,s}^{\min}$, and $c_{t,k,s}^{\max}$ characterize the step-wise linear real-time price quota curve $\phi_{t,k}(y_{t,k})$. For example, based on the curves in Figs. 1 and 2, we have $b_{t,k,1}^{\max} = 8$, $b_{t,k,2}^{\max} = 7$, $b_{t,k,3}^{\max} = 5$, etc.

### 4.3.2 Resulted Mixed-Integer Linear Program

After applying the changes in the four steps in Section 4.3.1, we can reformulate optimization problem (4.1) as

$$
\begin{aligned}
\textbf{min}\ & \frac{1}{K}\sum_{k=1}^{K}\sum_{t=\alpha}^{\beta} C_{t,k} + \sum_{s=1}^{o_{t,k}} \phi_{t,k,s}\left(c_{t,k,s} + w_{t,k,s} y_{t,k,s}^{\min}\right) \\
\textbf{s.t.}\ & \sum_{t=\alpha}^{\beta} q_{t,k} + y_{t,k} = e, && \forall k, \\
& x_t - \theta_{t,k} L \le q_{t,k}, && \forall t,k, \\
& q_{t,k} \le x_t, && \forall t,k, \\
& q_{t,k}^{\text{th}} - (1-\theta_{t,k})L \le q_{t,k}, && \forall t,k, \\
& q_{t,k} \le q_{t,k}^{\text{th}}, && \forall t,k, \\
& \sum_{s=1}^{m_{t,k}} \lambda_{t,k,s}\left(b_{t,k,s} + v_{t,k,s} x_{t,k,s}^{\min}\right) - \theta_{t,k} L \le C_{t,k}, && \forall t,k, \\
& C_{t,k} \le \sum_{s=1}^{m_{t,k}} \lambda_{t,k,s}\left(b_{t,k,s} + v_{t,k,s} x_{t,k,s}^{\min}\right), && \forall t,k, \\
& \sum_{s=1}^{n_{t,k}} x_{t,k,s}^{\min}\left(c_{t,k,s} + v_{t,k,s} p_{t,k,s}^{\min}\right) - (1-\theta_{t,k})L \le C_{t,k}, && \forall t,k, \\
& C_{t,k} \le \sum_{s=1}^{n_{t,k}} x_{t,k,s}^{\min}\left(c_{t,k,s} + v_{t,k,s} p_{t,k,s}^{\min}\right), && \forall t,k, \\
& q_{t,k}^{\text{th}} = \sum_{i=1}^{n_{t,k}} x_{t,k,s}^{\min} u_{t,k,s}, && \forall t,k, \\
& p_t = \sum_{i=1}^{n_{t,k}} \left(a_{t,k,s} + u_{t,k,s} p_{t,k,s}^{\min}\right), && \forall t,k, \\
& x_t = \sum_{s=1}^{m_{t,k}} \left(b_{t,k,s} + v_{t,k,s} x_{t,k,s}^{\min}\right), && \forall t,k, \\
& y_{t,k} = \sum_{s=1}^{o_{t,k}} \left(c_{t,k,s} + w_{t,k,s} y_{t,k,s}^{\min}\right), && \forall t,k, \\
& 0 \le a_{t,k,s} \le u_{t,k,s} a_{t,k,s}^{\max}, && \forall t,k,s,
\end{aligned}
\tag{4.42}
$$

$$
\begin{aligned}
&0 \leq b_{t,k,s} \leq v_{t,k,s} b^{\max}_{t,k,s}, && \forall t, k, s, \\
&0 \leq c_{t,k,s} \leq w_{t,k,s} c^{\max}_{t,k,s}, && \forall t, k, s, \\
&\sum_{s=1}^{n_{t,k}} u_{t,k,s} = 1, && \forall t, k, \\
&\sum_{s=1}^{m_{t,k}} v_{t,k,s} = 1, && \forall t, k, \\
&\sum_{s=1}^{o_{t,k}} w_{t,k,s} = 1, && \forall t, k, \\
&u_{t,k,s}, w_{t,k,s}, v_{t,k,s} \in \{0, 1\}, && \forall t, k, s,
\end{aligned}
$$

where the optimization variables are $x_t$, $p_t$, $y_{t,k}$, $\theta_{t,k}$, $q_{t,k}$, $q^{\text{th}}_{t,k}$, $C_{t,k}$, $a_{t,k,s}$, $b_{t,k,s}$, $c_{t,k,s}$, $u_{t,k,s}$, $v_{t,k,s}$, and $w_{t,k,s}$ for any time slot $t$, any market scenario $k$, and any step number $s$. The problem in (4.42) is a mixed-integer linear program.

## 4.4 More Complex Time-shiftable Loads

The model that we used in our analysis so far describes a time-shiftable load in its most generic form. In this section, we explain how other characteristics of time-shiftable loads can also be incorporated into the analysis. More specifically, we show that the optimal bidding framework in this section can include any other feature of time-shiftable loads, as long as the feature can be modeled as linear mixed-integer constraints.

### 4.4.1 Per-Time-Slot Consumption Limits

Some time-shiftable loads may have limitations on their consumption level at each time slot. Let $Z^{\min}$ and $Z^{\max}$ denote the minimum and maximum consumption levels that the time-shiftable load of interest can support. We must have

$$
Z^{\min} r_{t,k} \leq z_{t,k} \leq Z^{\max} r_{t,k} \quad \forall t, \ \forall k, \tag{4.43}
$$

where for each time slot $t$ and random scenario $k$, we have

$$z_{t,k} = q_{t,k} + y_{t,k} \tag{4.44}$$

and $r_{t,k}$ is a new binary variable to indicate whether the load is switched 'on' or 'off' at time slot $t$ and under scenario $k$.

### 4.4.2 Ramp Constraints

The ramp up and ramp down constraints do not allow the time-shiftable load to change its consumption level faster than certain rates within two consecutive time slots:

$$z_{t,k} - z_{t-1,k} \leq U^{max} \quad \forall t \geq 2, \ \forall k \tag{4.45a}$$

$$z_{t-1,k} - z_{t,k} \leq D^{max} \quad \forall t \geq 2, \ \forall k \tag{4.45b}$$

where $U^{max}$ and $D^{max}$ denote the maximum ramp up and maximum ramp down rates, respectively. Note that, the constraints in (4.45) address one type of *inter-temporal dependency* in time-shiftable loads. Another type is discussed next.

### 4.4.3 Uninterruptible Loads

If a time-shiftable load is *uninterruptible*, then as soon as it switches 'on' to start operation, it must continue its operation until it finishes its intended task. Based on the notations that we defined in Section 4.4.1, the following constraints must hold for an uninterruptable time-shiftable load:

$$r_{t,k} \leq r_{t+1,k} + \frac{1}{e} \sum_{\tau=1}^{t} z_{\tau,k} \quad \forall t \leq T-1, \ \forall k. \tag{4.46}$$

From (4.46), at time slot $t$ and under scenario $k$, we can choose $r_{t,k} = 1$ only if either $r_{t+1,k} = 1$, i.e., the operation of the load continues in the next time slot, or $\sum_{\tau=1}^{t} z_{\tau,k} = e$,

i.e., the operation of the load finishes by the end of the current time slot [24]. Note that, the constraints in (4.46) address yet another type of inter-temporal dependency in time-shiftable loads.

### 4.4.4 Aggregated Small Sub-Loads

In some cases, a time-shiftable load may consist of several smaller time-shiftable subloads or subtasks [45]. In that case, besides selecting the day-ahead and real-time market bids, we must also optimally schedule the operation of all subloads. Let $S \geq 1$ denote the number of time-shiftable subloads. For each subload $s = 1, \ldots, S$, let $\alpha_s$ and $\beta_s$ denote the beginning and the end of the time interval at which the subload can be scheduled. Also let $e_s$ denote the total energy that must be consumed in order to finish the operation of subload $s$. We can incorporate the problem of scheduling subloads by adding the following constraints into the problem formulation:

$$\sum_{s=1}^{S} z_{t,k,s} = z_{t,k} \quad \forall t,\ \forall k, \tag{4.47}$$

$$\sum_{t=\alpha_l}^{\beta_l} z_{t,k,s} = e_l \quad \forall s,\ \forall k. \tag{4.48}$$

Note that, if there is only one subload, i.e., $S = 1$, then (4.47) reduces to (4.44); and (4.48) reduces to the first constraint in (4.42).

## 4.5 Case Studies

### 4.5.1 Case Study 1: A Detailed Illustrative Example

In this section, we present a detailed illustrative example. Suppose we would like to procure energy for a time-shiftable load with start time $\alpha = 1$, deadline $\beta = T = 3$, and total energy consumption $e = 75$ MWh. The uncertainty in the electricity market is modeled using $K = 2$ scenarios.

**Basic Time-Shiftable Loads**

First, consider the most generic time-shiftable load model. The price quota curves for the day-ahead and the real-time markets and the corresponding optimal bids are shown in Fig. 4.3. These optimal solutions are first obtained by solving the mixed-integer linear program in (4.42) and then the results are verified using exhaustive search. Using a computer with a 2.40 GHz CPU and 80 GB shared RAM, the mixed-integer linear program in (4.42) was solved in *less than 1 second*. However, it took *multiple days* for the exhaustive search with several *for loops* to finish the search and give the exact same solution.

From Fig. 4.3, we can see that the bidding outcome and the schedule of the time-shiftable load across time slots highly depends on the realization of the market scenario. For example, if scenario $k = 1$ occurs, then the power consumption at time slot $t = 1$ becomes 47 MWh, out of which 20 MWh is procured from the day-ahead market at 24 \$/MW and 27 MWh is procured from the real-time market at 29 \$/MW. In this scenario, because the prices are high at time slot $t = 2$, no energy usage is scheduled at this time slot. Finally, the power consumption at time slot $t = 3$ and scenario $k = 1$ is $75 - 47 = 28$ MWh, out of which 10 MWh is procured from the day-ahead market at 23 \$/MW and 18 MWh is procured from the real-time market at 25 \$/MW. The total cost of power purchase from the day-ahead market in this scenario is $C_{1,1} + C_{2,1} + C_{3,1} = 20 \times 24 + 0 \times 0 + 10 \times 23 =$ \$710. Also, the total cost of power procurement from the real-time market is obtained as $27 \times 29 + 0 \times 0 + 18 \times 25 =$ \$1,233.

We can similarly calculate the total cost of power procurement from the day-ahead market and the total cost of power procurement from the real-time market under scenario $k = 2$ as \$1,089 and \$708, respectively. Therefore, the *expected overall cost of power procurement*, i.e., the objective value in optimization problem (4.1) becomes \$1,870. Note that if we use the price-maker Self-Schedule bidding in [72], then the total expected cost of power procurement becomes \$1,904, i.e., \$34 higher than our proposed price-maker

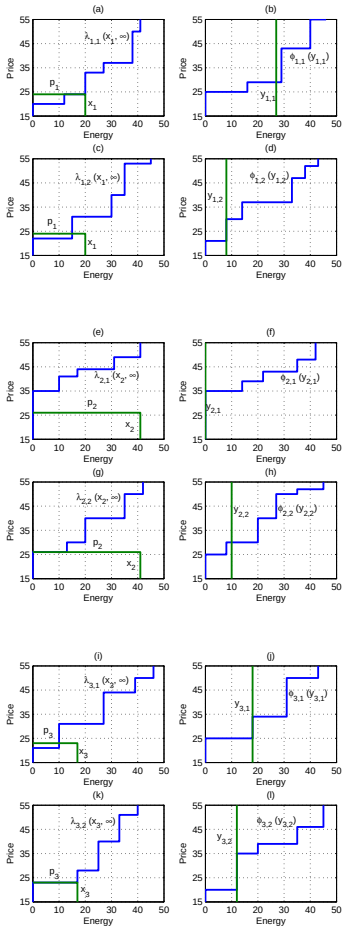


Figure 4.3: The price quota curves and optimal bids for Case Study 1, where the time-shiftable load has its basic features. Sub-figures (a), (c), (e), (g), (i), (k) correspond to the day-ahead market and sub-figures (b), (d), (f), (h), (j), (l) correspond to the real-time market.

economic bidding method. Also, if we do *even load distribution*, i.e., we distribute the total load $e = 75$ MWh equally across the $\beta - \alpha + 1 = 3$ time-slots and also equally across the day-ahead and real-time markets, then the total expected cost of power procurement becomes \$2,169, i.e., \$299 higher than our proposed price-maker economic bidding method.

### Time-Shiftable Loads with Consumption Limits

Next, we consider the basic time-shiftable load model, but we also assume that there exist per-time-slot consumption limits as in Section 4.4.1. The results are shown in Fig. 4.4(a), where $Z^{\min} = 0$ MWh and $Z^{max}$ varies from 25 to 50 MWh. We can see that the optimal energy procurement cost is high if the operation of the time-shiftable load is highly restricted due to the per-time-slot power consumption constraints. However, as we increase $Z^{max}$, the cost reduces and finally reaches its original level as in previous example, where $Z^{\max}$ is not binding.

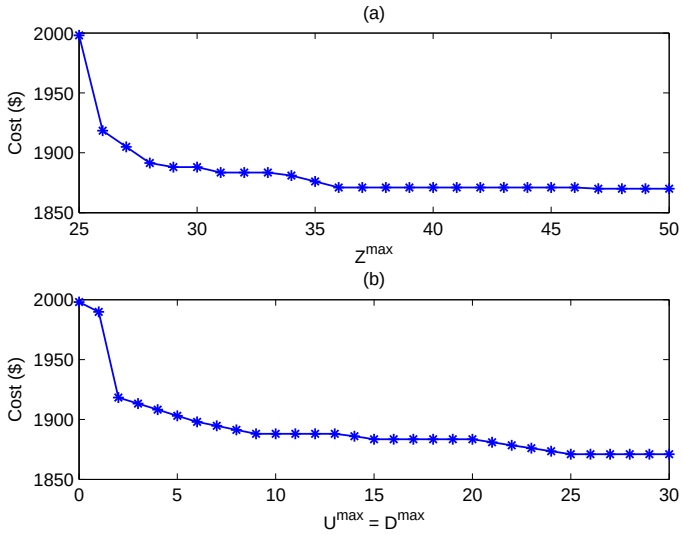


Figure 4.4: The cost of energy procurement for Case Study 1 when the time-shiftable has (a) per-time-slot consumption limits; (b) ramp constraints.

### Time-Shiftable Loads with Ramp Constraints

Again, consider the basic time-shiftable load model, but this time assume that there exist ramp constraints as in Section 4.4.2. The results are shown in Fig. 4.4(b), where $U^{max} = D^{max}$ vary from 0 to 30 MWh. Note that, if $U^{max} = D^{max} = 0$, then the load does not tolerate any inter-temporal variation. We can see that ramp constraints

can significantly increase the energy procurement cost. However, as we increase $U^{max}$ and $D^{max}$, the cost reduces and finally reaches its original level as in the original example, where the ramp constraints are not binding.

**Uninterruptible Time-Shiftable Loads**

Recall from Section 4.4.3 that if a time-shiftable load is uninterruptible, then it is still flexible with respect to its operation start time; however, once it starts operation, it cannot be interrupted until it finishes its task. Here, interruption is defined as selecting $z_{t,k} < Z^{\min}$, which requires choosing $r_{t,k} = 0$, i.e., switching the load off. The optimal bids when the time-shiftable load is uninterruptible is shown in Fig. 4.5, where $Z^{\min} = 15$. We can see that, the time-shiftable load procures energy from all three time slots, including the second time slot which has high prices. This is because, unlike in Fig. 4.3, here, the operation cannot be interrupted during the second time slot and then resumed during the third time slot. Note that, since an uninterruptible time-shiftable load is less flexible than a basic time-shiftable load, it pays 14$ more for its energy procurement compared to the first example.

**Aggregated Time-shiftable Subloads**

To study the impact of time-shiftable subloads on the choice of demand bids, the total load $e = 75$ MWh is now divided into three sub-loads as follow: 1) $e_1 = 10$, $\alpha_1 = 1$, $\beta_1 = 3$, 2) $e_2 = 20$, $\alpha_2 = 1$, $\beta_2 = 2$, and 3) $e_3 = 45$, $\alpha_3 = 2$, $\beta_3 = 3$. Fig. 4.6 shows the procured energy for different loads at scenarios $k = 1$ and $k = 2$. We can see that the different start and end-times for sub-loads affects the amount of total energy that needs to be procured under each scenario and at each time slot.

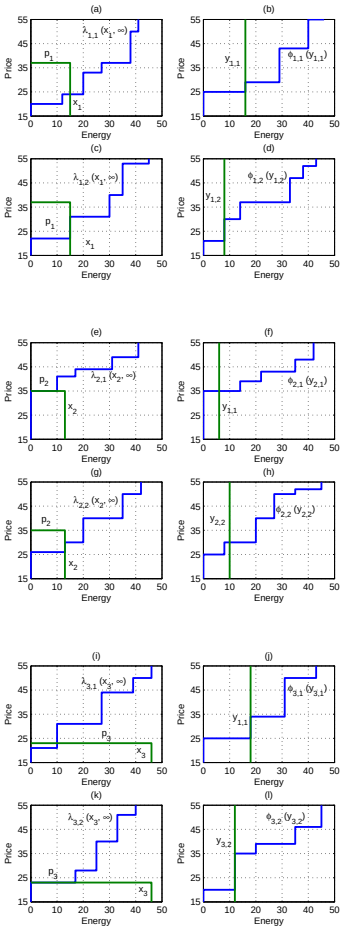


Figure 4.5: The price quota curves and optimal bids for Case Study 1, where the time-shiftable load uninterrupitble as addressed in Section 4.5.1. Sub-figures (a), (c), (e), (g), (i), (k) correspond to the day-ahead market and sub-figures (b), (d), (f), (h), (j), (l) correspond to the real-time market.

### 4.5.2 Case Study 2: California Energy Market

In this section, we present some additional case studies, this time based on the California energy market. To create the price quota curves, we used the hourly generator bids data from the public bids database in [61] at one dollar price bid resolution. The day-ahead and real-time prices are also obtained from the prices database in [61], where we averaged real-time market prices in each hour to make them comparable with the hourly price data from the day-ahead market. Finally, since the focus in this section is on pool-

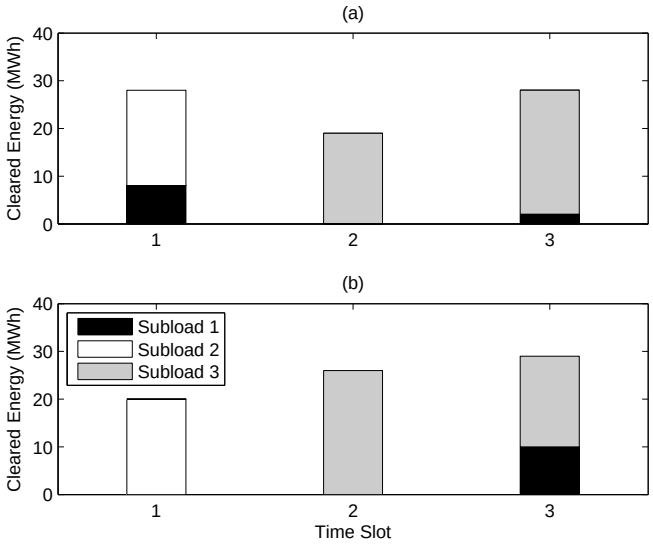


Figure 4.6: The procured energy for different time-shiftable sub-loads at different time slots as in Section 4.5.1: (a) scenario $k = 1$, (b) scenario $k = 2$.

based markets, the grid topology and transmission constraints are not considered in our simulations.

In total, we examined 10 cases. Each case has a time shiftable load with $E = 10$ GWh and $K = 3$ market scenarios. For Case 1, the three scenarios are based on the price and bid data during January 1, 2014 to January 3, 2014. For Case 2, the three scenarios are based on the price and bid data during January 4, 2014 to January 6, 2014. The rest of the cases are setup similarly, all together using data for 30 days. For each case, three design options are compared: 1) Optimal price-marker self-schedule bidding, which is an extension of the design in [72] to both day-ahead and real-time markets; 2) Optimal price-marker economic bidding, which is based on the design in this section; and 3) Even load distribution, which distributes the load equally across time-slots and markets.

The amount of savings due to using optimal price-maker economic bidding over optimal price-maker self-schedule bidding across the 10 cases are shown in Figs. 4.7(a) and (b), during some off-peak hours from $\alpha =$ 10:00 AM to $\beta =$ 12:00 PM and also during some on-peak hours from $\alpha =$ 15:00 PM to $\beta =$ 17:00 PM, receptively. Similarly, the amount

of savings due to using optimal price-maker economic bidding over even load distribution across the 10 cases are shown in Fig. 4.8.

Finally, the detailed simulation results for the example of Case 1 during off-peak hours are shown in Figs. 4.9 and 4.10. We can see major differences across the three designs, in terms of both the average cleared energy and the average purchase price. Note that, the averaging here is done across the $K = 3$ random market scenarios. For instance, on average, if optimal price-maker economic bidding is employed, then 29.8%, 33.7% and 36.5% of the total needed energy is purchased from the day-ahead and real-time markets during hours 10:00 AM, 11:00 AM, and 12:00 PM, respectively. These percentages change to 30.6%, 38.1% and 21.3% if optimal price-maker self-scheduling is being employed. As for the price results in Fig. 10, an interesting observation is that optimal price-maker economic bidding is more successful in *smoothing down* the prices across the three operational hours and also to some extent across the day-ahead and real-time markets.

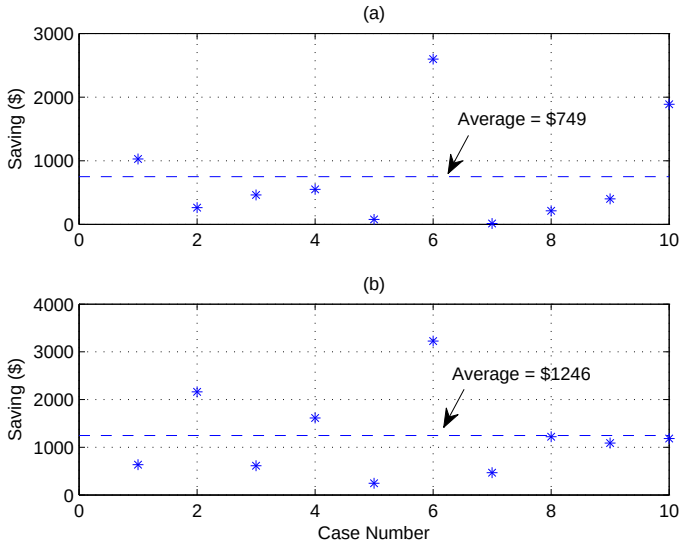


Figure 4.7: Savings due to using optimal price-maker economic bidding over optimal price-maker self-scheduling: (a) off-peak hours, (b) peak hours.

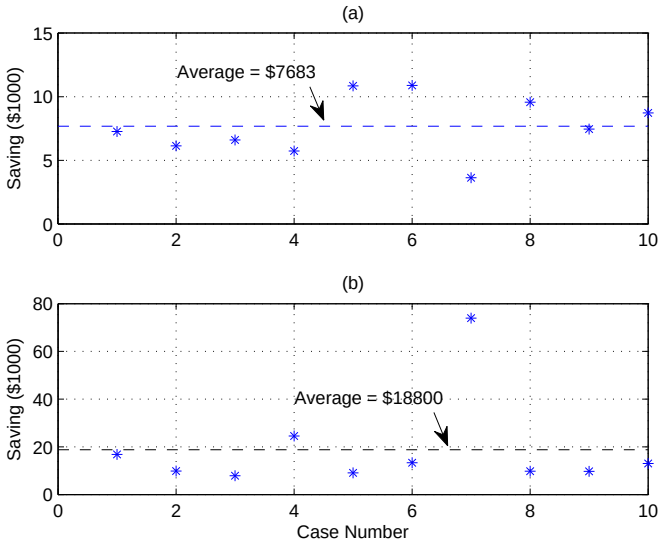


Figure 4.8: Savings due to using optimal price-maker economic bidding over even load distribution: (a) off-peak hours, (b) peak hours.

Finally, the computation time of the proposed method versus the number of random scenarios is shown in Table 4.1. As one would expect, increasing the number of random scenarios results in increasing the number of optimization variables, i.e., increasing the size of the optimization problem. Accordingly, the computation time increases. When it comes to solving mixed-integer linear programs, the computation time particularly depends on the number of binary variables, because it indicates the maximum branching steps needed when we use a branch and bound algorithm [81]. From Table 4.1, despite the increased computational complexity, one can still use the proposed method in this section under larger sets of random scenarios. If needed, one can lower the price resolution at price quota curve, e.g., by setting resolution to $2 instead of $1, so as to decrease the number of steps in the price quota curve in order to further lower the computation time.

## 4.6 Conclusions

We formulated and efficiently solved a new scenario-based stochastic mixed-integer linear programming framework for price-maker economic bidding of time-shiftable loads

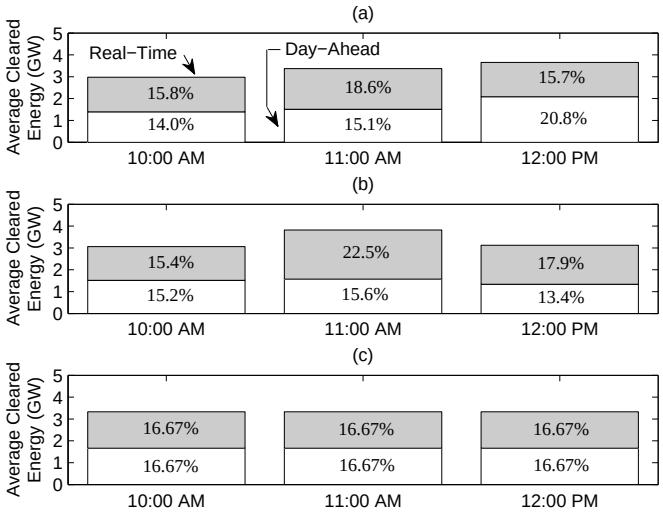


Figure 4.9: Comparison between the three designs in terms of average cleared energy for Case 1 during off-peak hours: (a) optimal price-maker economic bidding, (b) optimal price-maker self-scheduling, (c) even load distribution.

with deadlines in day-ahead and real-time markets. On the application side, the results in this section extended some recent results in price-taker operation of time-shiftable loads in wholesale electricity markets. Both basic and complex time-shiftable load types are addressed, where the latter includes time-shiftable loads that are uninterruptible, have per-time-slot consumption limits or ramp constraints, or comprise several smaller time-shiftable subloads. On the methodology side, the results in this section also extended the existing results on price-maker self-scheduling of both loads and generators, because price-maker self-scheduling is a restricted special case of price-maker economic bidding. To investigate the performance of our design, a highly detailed illustrative case study along with multiple case studies based on the California energy market data are presented. We showed that the proposed optimal price-maker economic bidding approach outperforms both optimal price-maker self-scheduling and even-load-distribution.

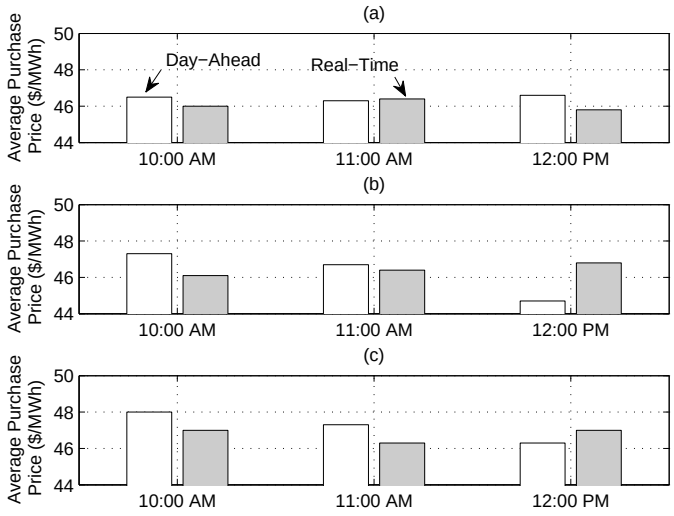


Figure 4.10: Comparison between the three designs in terms of average purchase price for Case 1 during off-peak hours: (a) optimal price-maker economic bidding, (b) optimal price-maker self-scheduling, (c) even load distribution.

Table 4.1: Computation time versus the number of scenarios

| # of Scenarios | # of Variables | # of Binary Variables | Computation Time (Sec) |
|---|---|---|---|
| 1 | 228 | 105 | 0.7 |
| 2 | 406 | 188 | 0.8 |
| 3 | 570 | 264 | 2.7 |
| 4 | 760 | 353 | 6.2 |
| 5 | 958 | 446 | 23 |
| 6 | 1080 | 501 | 37 |
| 7 | 1214 | 562 | 91 |
| 8 | 1422 | 660 | 289 |
| 9 | 1616 | 751 | 897 |
| 10 | 1804 | 839 | 1478 |

# Chapter 5

# Analysis of Convergence Bids in Nodal Electricity Markets

## 5.1 Introduction

Ideally, and to assure market efficiency, there must be no difference between the prices in the day-ahead market (DAM) and the real-time market (RTM). Otherwise, some generation resources may practice market power and withhold a portion of their capacities to increase the DAM or RTM prices to gain more profit [26–28, 82].

Nevertheless, in practice, there is always a *gap* between the two sets of prices. For example, Fig. 5.1(b) shows the distribution of the price difference in trading hub SP15 in Southern California across 24 hours and 30 days in March 2016 [61]. Here, the price difference is calculated as the DAM price minus the RTM price. There are several days and hours (such as 2 PM on March 14) where the DAM price is much higher than the RTM price and there are also several days and hours (such as 9 AM on March 14) where the RTM price is much higher than the DAM price. Fig. 5.1(c) shows similar data at two nodes within SP15 on March 8 and 14. We can see that price gap can be less or more severe

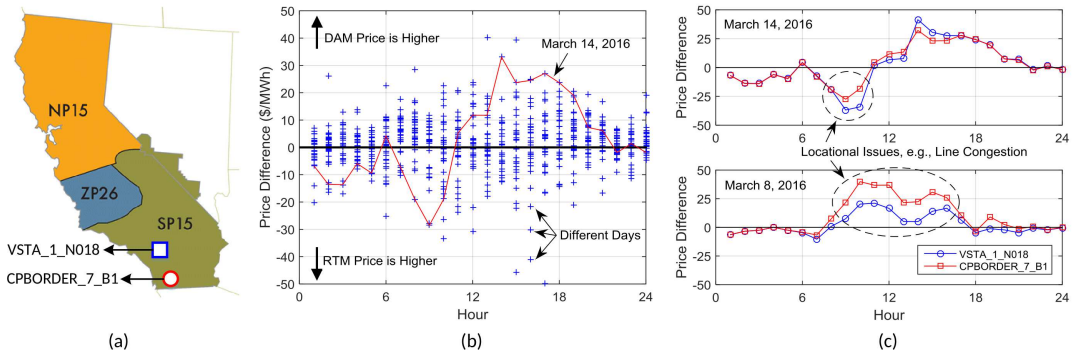


Figure 5.1: Examples of the price gap, i.e., the DAM price minus the RTM price, in the California ISO market during March 2016: (b) the full month for trading hub SP15 in Southern California; (c) two sample days at two nodes within SP15.

at different nodes due to locational issues such as transmission line congestion.

### 5.1.1 Convergence Bidding Concept

To eliminate the above price gap, Convergence bids (CBs), a.k.a., Virtual bids (VBs), have been introduced to electricity markets [26–28]. Note that, CB is the term that is used by the California ISO and VB is the term that is used by the Pennsylvania-Jersey-Maryland (PJM) Interconnection and some other ISOs. CBs allow market participants to arbitrage between the DAM and RTM, exempting them from physically consuming or producing energy [27]. CBs are similar to what is known as future trading in traditional commodity and financial markets [26]. Similar to physical bids, CBs have two types: supply CBs and demand CBs. Supply (demand) CB is a bid to sell (buy) energy in DAM without any obligation to produce (consume) energy. If the CB is cleared in the DAM, then the bidder is credited (charged) at the DAM price and charged (credited) at the RTM price. Therefore, the difference between the earning in the DAM (RTM) and the cost in the RTM (DAM) will be the payment to the CB bidder.

From an ISO's perspective, if participants make profit through CBs, it should automatically help closing the price gap [53]. For example, when DAM price is greater (less) than the RTM price, the participants can make profit by submitting supply (demand) CB

into DAM. Increasing supply (demand) CBs results in decreasing (increasing) the DAM price due to the virtual surplus of supply (demand) in the DAM. As a result, more (less) demand needs to be cleared in the RTM leading to increase (decrease) in the RTM price [26, 53, 58]. Therefore, while market participants make profit out of their CBs, they also help in reducing the price difference between the DAM and RTM; thus, solving the aforementioned price gap problem.

### 5.1.2 Concerns about Convergence Bids' performance

The concept of CBs is relatively new in the ISO markets. For example, California ISO put CBs into effect in 2011 [59]. So far, most ISOs have adopted this concept with almost no rudimentary changes from traditional commodity and financial markets [58]. However, there are recent ISO reports raising some concerns about CBs, arguing that CBs may not have performed well in ISO markets and it is generally difficult for ISOs to even analyze how CBs may have actually affected price convergence and market efficiency in ISO markets. For example, here is a related quote from the California ISO 2015 Annual Report on Market Issues and Performance [57]:

> "However, the degree to which convergence bidding has actually increased market efficiency has not been assessed. In some cases, virtual bidding may be profitable for some market participants without increasing market efficiency significantly or even decreasing market efficiency."

Here is another quote from the PJM Interconnection 2015 Report on Virtual Transactions in the Energy Markets [58]:

> "In considering when and to what degree virtual trading offers benefits to PJM markets, it is important to account for these distinctions before definitively concluding that the generally accepted principles of market efficiency as demonstrated by trading in other financial and commodity marketplaces hold equally well to PJM's energy markets."

The above citations and quotes exemplify the current state of uncertainty and debate about the advantages or disadvantages of CBs in nodal electricity markets. With this in mind, our study seeks to address the above open problem by analyzing how a CB may affect the price gap between DAM and RTM.

### 5.1.3 Our Goal

In this section, we focus on one of the primary factors that influence the performance of CBs in electricity markets, i.e., transmission line congestion. Our goal is to provide in-depth sensitivity analysis to undestrant how the price gap between DAM and RTM is affected by the CBs under different grid operational conditions in congested nodal electrcity markets. Our analysis is *not* statistical; thus, it is inherently different from the existing literature on CBs in electricity markets, e.g., in [83–86]. Instead, we look at the basic formulation of CBs in nodal electricity markets and obtain *closed-form* sensitivity models to explain how a CB may influence the DAM and RTM prices at a bus where it is cleared. Finally, built upon the fundamental sensitivity analysis, several case studies are presented to show that the impact of CBs in the nodal electricity market may cause price convergence (intuitive result) or price divergence (counter-intuitive result).

## 5.2 Sensitivity Analysis of Two-Settlement Market Prices to Convergence Bids

In this section, we investigate the sensitivity of the DAM and RTM prices to CBs in order to understand how CBs may influence the price difference in a two-settlement nodal electricity market.

### 5.2.1 Electricity Market Model

Consider the following DAM market clearing optimization problem in presence of convergence bids [27, 85]:

$$\textbf{min} \quad 0.5\,\mathbf{p}^T\mathbf{A}\mathbf{p} + \mathbf{b}^T\mathbf{p} \tag{5.1a}$$

$$\textbf{s.t.} \quad \mathbf{1}^{\mathrm{T}}\,\mathbf{p} = 0 \qquad : \lambda \tag{5.1b}$$

$$-\mathbf{c} \leq \mathbf{S}\,\mathbf{\Phi}\,\mathbf{p} \leq \mathbf{c} \quad : \boldsymbol{\mu}^-, \boldsymbol{\mu}^+ \tag{5.1c}$$

$$\mathbf{p}^{\min} \leq \mathbf{p} \leq \mathbf{p}^{\max} \tag{5.1d}$$

where the optimization variables are

$$\mathbf{p} \triangleq \begin{bmatrix} \mathbf{x} & \mathbf{y} & \mathbf{v} & \mathbf{w} \end{bmatrix}^{\mathrm{T}}. \tag{5.2}$$

In (5.1), $\mathbf{A}$ is a positive diagonal matrix comprising $\alpha$ and $-\alpha$ components of all supply and demand bids in the DAM, respectively. Both physical and convergence bids are taken into consideration. Moreover, $\mathbf{b}$ is the vector comprising of $\beta$ and $-\beta$ components of all supply and demand bids, respectively. Equality (5.1b) represents the system balance constraint ensuring total generation matches total load. Also, the Lagrange multiplier associated with (5.1b) provides the reference price. The transmission line flow limit constraints in two directions are expressed in (5.1c). Also, the Lagrange multipliers associated with (5.1c) indicate the shadow prices. The last inequality in (5.1d) expresses each participant's upper and lower operating capacity limits. Finally, by using the reference and shadow prices, the LMPs can be obtained as

$$\boldsymbol{\pi} = \lambda\mathbf{1} - \mathbf{S}^T\boldsymbol{\mu}, \quad \text{where } \boldsymbol{\mu} = \boldsymbol{\mu}^+ - \boldsymbol{\mu}^-. \tag{5.3}$$

The RTM market clearing optimization problem can also be formulated as [27,85]:

$$\textbf{min} \quad 0.5\,\mathbf{z}^T\mathbf{C}\,\mathbf{z} + \mathbf{d}^T\mathbf{z} \tag{5.4a}$$

$$\textbf{s.t.} \quad \mathbf{1}^T\mathbf{z} + \mathbf{1}^T\mathbf{x} = \mathbf{1}^T\boldsymbol{l} \qquad : \delta \tag{5.4b}$$

$$-\mathbf{c} \leq \mathbf{S}(\boldsymbol{\Psi}\,\mathbf{x} + \boldsymbol{\Theta}\,\mathbf{z} - \boldsymbol{\Omega}\,\boldsymbol{l}) \leq \mathbf{c} \quad : \boldsymbol{\eta}^-, \boldsymbol{\eta}^+ \tag{5.4c}$$

$$\mathbf{z}^{\min} \leq \mathbf{z} \leq \mathbf{z}^{\max} \tag{5.4d}$$

where the optimization variables are the elements of vector $\mathbf{z}$. Similar to the DAM LMPs, the RTM LMPs are obtained by using the Lagrange multipliers in (5.4b) and (5.4c) as

$$\boldsymbol{\sigma} = \delta\mathbf{1} - \mathbf{S}^T\boldsymbol{\eta}, \quad \text{where } \boldsymbol{\mu} = \boldsymbol{\eta}^+ - \boldsymbol{\eta}^-. \tag{5.5}$$

We must note two key differences between (5.1) and (5.4). First, demand bids are not allowed at the RTM, instead, ISOs use the forecasted load as constant at problem (5.4), c.f. [60]. Second, as in practice, the RTM clearing process is based on only physical bids but *not* CBs [27,85]. Note that, even though CBs do not appear in the RTM optimization in (5.4), because they *do* affect the cleared physical supply bids in the DAM i.e. $\mathbf{x}$, they indirectly have impact on the LMPs of the RTM.

### 5.2.2 Closed-Form Sensitivity Analysis

We are now ready to present a formal theorem to explain how the cleared energy of a CB can affect price difference between the DAM and RTM at the bus where the CB is placed.

**Theorem 1** *Consider a CB at bus $i$. Without loss of generality, suppose it s a supply CB, whose cleared energy bid is denoted by $\boldsymbol{v}_i$. (a) The price gap $\boldsymbol{\Delta}_i = \boldsymbol{\pi}_i - \boldsymbol{\sigma}_i$ at bus $i$ is a piecewise linear function of the cleared CB ($\boldsymbol{v}_i$). (b) The slope of such function, i.e., the*

*right-sided partial derivative, is obtained as*

$$\begin{aligned}\frac{\partial \boldsymbol{\Delta}_i}{\partial \boldsymbol{v}_i} &= \frac{\partial \boldsymbol{\pi}_i}{\partial \boldsymbol{v}_i} - \frac{\partial \boldsymbol{\sigma}_i}{\partial \boldsymbol{v}_i} \\ &= \frac{-1}{\boldsymbol{1}^T \boldsymbol{h}} - \frac{1}{\boldsymbol{1}^T \boldsymbol{e}} \frac{1}{\boldsymbol{1}^T \boldsymbol{h}} (\boldsymbol{1}^T \hat{\boldsymbol{K}} \boldsymbol{h} - \boldsymbol{r} \hat{\boldsymbol{K}} \boldsymbol{h}) \\ &= -\frac{1}{\boldsymbol{1}^T \boldsymbol{h}} \frac{1}{\boldsymbol{1}^T \boldsymbol{e}} (\boldsymbol{1}^T \boldsymbol{e} + \boldsymbol{1}^T \hat{\boldsymbol{K}} \boldsymbol{h} - \boldsymbol{r} \hat{\boldsymbol{K}} \boldsymbol{h}),\end{aligned} \tag{5.6}$$

*where*

$$\boldsymbol{h} \triangleq \boldsymbol{\Lambda} \boldsymbol{1} - \boldsymbol{\Lambda} \boldsymbol{X}^T (\boldsymbol{X} \boldsymbol{\Lambda} \boldsymbol{X}^T)^{-1} \boldsymbol{X} \boldsymbol{\Lambda} \boldsymbol{1}, \tag{5.7}$$

$$\boldsymbol{e} \triangleq \boldsymbol{\Gamma} \boldsymbol{1} - \boldsymbol{\Gamma} \boldsymbol{Y}^T (\boldsymbol{Y} \boldsymbol{\Gamma} \boldsymbol{Y}^T)^{-1} \boldsymbol{Y} \boldsymbol{\Gamma} \boldsymbol{1}, \tag{5.8}$$

$$\boldsymbol{r} \triangleq \boldsymbol{1}^T \boldsymbol{\Gamma} \boldsymbol{Y} (\boldsymbol{Y} \boldsymbol{\Gamma} \boldsymbol{Y}^T)^{-1} \bar{\boldsymbol{R}} \boldsymbol{S} \hat{\boldsymbol{\Psi}}, \tag{5.9}$$

*and* $\boldsymbol{\Lambda}$, $\boldsymbol{\Gamma}$, $\hat{\boldsymbol{K}}$, $\boldsymbol{X}$, $\boldsymbol{Y}$, $\bar{\boldsymbol{R}}$, *and* $\hat{\boldsymbol{\Psi}}$ *are constant matrices that depend on cleared bids and admittance and congestion status of lines.*

Note that, if the CB is a demand bid, then we can replace $\mathbf{v}_i$ with $-\mathbf{w}_i$ in (5.6). The proof of Theorem 1 is as follows.

**Proof.** Suppose bus $i$ is taken as the reference bus, the price gap at bus $i$ is obtained as $\boldsymbol{\Delta}_i = \lambda - \delta$. Let $\mathbf{v}_{-i}$ denote the set of all supply CBs other than $\mathbf{v}_i$. We can now define:

$$\mathbf{p}_{-i} \triangleq \begin{bmatrix} \mathbf{x} & \mathbf{y} & \mathbf{v}_{-i} & \mathbf{w} \end{bmatrix}^{\mathrm{T}} \tag{5.10}$$

as the optimal solution of all variables in (5.1) other than $\mathbf{v}_i$. We also define $\mathbf{A}_{-i}$, $\mathbf{b}_{-i}$, $\mathbf{p}_{-i}^{\min}$, $\mathbf{p}_{-i}^{\max}$, and $\boldsymbol{\Phi}_{-i}$ by removing row $i$ and/or column $i$ from $\mathbf{A}$, $\mathbf{b}$, $\mathbf{p}^{\min}$, $\mathbf{p}^{\max}$, and $\boldsymbol{\Phi}$.

Let us now decompose vector $\mathbf{p}_{-i}$ into vector $\bar{\mathbf{p}}_{-i}$ for entries that are *binding* by any of the two inequality constraints in (5.1d) and vector $\hat{\mathbf{p}}_{-i}$ for entries that are *not* binding by either of these two constraints. Similarly, we define $\bar{\mathbf{A}}_{-i}$, $\hat{\mathbf{A}}_{-i}$, $\bar{\mathbf{b}}_{-i}$, $\hat{\mathbf{b}}_{-i}$, $\bar{\mathbf{p}}_{-i}^{\min}$, $\hat{\mathbf{p}}_{-i}^{\min}$, $\bar{\mathbf{p}}_{-i}^{\max}$, $\hat{\mathbf{p}}_{-i}^{\max}$, $\bar{\boldsymbol{\Phi}}_{-i}$, and $\hat{\boldsymbol{\Phi}}_{-i}$. We also decompose vector $\boldsymbol{\mu}$ into vector $\bar{\boldsymbol{\mu}}$ for the Lagrange multipliers corresponding to the *binding* constraints in (5.1c). Let $\bar{\mathbf{D}}$ denote a row-reduced identity

matrix, i.e., an identity matrix with the same size of matrix $\mathbf{S}$ whose rows that correspond to the non-binding transmission line capacity constraints are eliminated. Finally, we define $\hat{\boldsymbol{\mu}}$ as the Lagrange multipliers which are *not* binding by any of the transmission line capacity constraints. Note that, due to complimentary slackness, we have $\hat{\boldsymbol{\mu}} = \mathbf{0}$. Using convex optimization theory [87, Chapter 4], we can show that problem (5.1) is *equivalent* to the following problem:

$$\min_{\hat{\mathbf{p}}_{-i}} \quad 0.5\, \hat{\mathbf{p}}_{-i}^T\, \hat{\mathbf{A}}_{-i}\, \hat{\mathbf{p}}_{-i} + \hat{\mathbf{b}}_{-i}^T\, \hat{\mathbf{p}}_{-i} \tag{5.11a}$$

$$\text{s.t.} \quad \mathbf{1}^T \hat{\mathbf{p}}_{-i} + \mathbf{1}^T \bar{\mathbf{p}}_{-i} + \mathbf{v}_i = 0 \qquad : \lambda \tag{5.11b}$$

$$\bar{\mathbf{D}}\mathbf{S}\, (\hat{\boldsymbol{\Phi}}_{-i}\, \hat{\mathbf{p}}_{-i} + \bar{\boldsymbol{\Phi}}_{-i}\, \bar{\mathbf{p}}_{-i}) = \bar{\mathbf{D}}\mathbf{c} \quad : \bar{\boldsymbol{\mu}}. \tag{5.11c}$$

Here, $\mathbf{v}_i$ and $\bar{\mathbf{p}}_{-i}$ are fixed at their optimal values but $\hat{\mathbf{p}}_{-i}$ is variable. The objective function includes only those terms that depend on $\hat{\mathbf{p}}_{-i}$. Since bus $i$ is the reference bus, $\mathbf{S}\boldsymbol{\Phi}\mathbf{p} = \mathbf{S}\boldsymbol{\Phi}_{-i}\mathbf{p}_{-i}$. Also, we kept only those line capacity constraints that are binding at the optimal solution of problem (5.1).

Since (5.11) is a convex quadratic program, it can be solved by equivalently solving the following system of linear equations, namely the KKT conditions [87], over $\hat{\mathbf{p}}_{-i}$, $\lambda$ and $\bar{\boldsymbol{\mu}}$, as follow:

$$\boldsymbol{\Lambda}^{-1}\hat{\mathbf{p}}_{-i} + \hat{\mathbf{b}}_{-i} = \begin{bmatrix} \mathbf{1}^T \\ -\mathbf{X} \end{bmatrix}^T \begin{bmatrix} \lambda \\ \bar{\boldsymbol{\mu}} \end{bmatrix} \tag{5.12a}$$

$$\begin{bmatrix} \mathbf{1}^T \\ \mathbf{X} \end{bmatrix} \hat{\mathbf{p}}_{-i} = \mathbf{n} - \begin{bmatrix} 1 \\ \mathbf{0} \end{bmatrix} \mathbf{v}_i. \tag{5.12b}$$

where

$$\mathbf{X} \triangleq \bar{\mathbf{D}}\mathbf{S}\hat{\boldsymbol{\Phi}}_{-i}, \quad \boldsymbol{\Lambda} \triangleq \hat{\mathbf{A}}_{-i}^{-1}, \quad \mathbf{n} \triangleq \begin{bmatrix} -\mathbf{1}^T \bar{\mathbf{p}}_{-i} \\ \bar{\mathbf{D}}\mathbf{c} - \bar{\mathbf{D}}\mathbf{S}\, \bar{\boldsymbol{\Phi}}_{-i}\, \bar{\mathbf{p}}_{-i} \end{bmatrix}. \tag{5.13}$$

The coefficients in (5.12) hold as long as the set of binding constraints do not change at the solution of problem (5.1). If a binding constraint becomes unbinding or an unbinding constraint becomes binding, then some or all matrices $\mathbf{\Lambda}$, $\hat{\mathbf{b}}_{-i}$, $\mathbf{X}$, and $\mathbf{n}$ may change, but keeping the relationship between variables, i.e., $\lambda$ and $\mathbf{v}_i$, linear. Thus, the overall relationship is piecewise linear. From (5.12) and (5.7), we have:

$$\partial\lambda/\partial\mathbf{v}_i = -1/\mathbf{1}^T\mathbf{h}. \tag{5.14}$$

The analysis of the RTM prices is similar. We can first show that problem (5.4) is *equivalent* to the following problem:

$$\min_{\hat{\mathbf{z}}} \quad 0.5\,\hat{\mathbf{z}}^T\hat{\mathbf{C}}\,\hat{\mathbf{z}} + \hat{\mathbf{d}}^T\hat{\mathbf{z}} \tag{5.15a}$$

$$\text{s.t.} \quad \mathbf{1}^T\hat{\mathbf{z}} + \mathbf{1}^T\bar{\mathbf{z}} + \mathbf{1}^T\hat{\mathbf{x}} + \mathbf{1}^T\bar{\mathbf{x}} = \mathbf{1}^T\boldsymbol{l} \quad : \delta \tag{5.15b}$$

$$\bar{\mathbf{R}}\mathbf{S}(\bar{\mathbf{\Psi}}\,\bar{\mathbf{x}} + \hat{\mathbf{\Psi}}\,\hat{\mathbf{x}} + \bar{\mathbf{\Theta}}\,\bar{\mathbf{z}} + \hat{\mathbf{\Theta}}\,\hat{\mathbf{z}} - \mathbf{\Omega}\,\boldsymbol{l}) = \bar{\mathbf{R}}\mathbf{c} \quad : \bar{\boldsymbol{\eta}}, \tag{5.15c}$$

where $\hat{\mathbf{x}} = \hat{\mathbf{K}}\,\hat{\mathbf{p}}_{-i}$ and $\bar{\mathbf{x}} = \bar{\mathbf{K}}\,\bar{\mathbf{p}}_{-i}$. Again, since (5.15) is a convex quadratic program, we can solve it by equivalently solving its corresponding KKT conditions [87], which in this case are a system of linear equations over $\hat{\mathbf{z}}$, $\delta$ and $\bar{\boldsymbol{\eta}}$:

$$\mathbf{\Gamma}^{-1}\hat{\mathbf{z}} + \hat{\mathbf{d}} = \begin{bmatrix} \mathbf{1}^T \\ -\mathbf{Y} \end{bmatrix}^T \begin{bmatrix} \delta \\ \bar{\boldsymbol{\eta}} \end{bmatrix} \tag{5.16a}$$

$$\begin{bmatrix} \mathbf{1}^T \\ \mathbf{Y} \end{bmatrix} \hat{\mathbf{z}} = \mathbf{m} - \begin{bmatrix} \mathbf{1}^T \\ \bar{\mathbf{R}}\mathbf{S}\hat{\mathbf{\Psi}} \end{bmatrix} \hat{\mathbf{K}}\hat{\mathbf{p}}_{-i} \tag{5.16b}$$

where $\mathbf{Y} \triangleq \bar{\mathbf{R}}\mathbf{S}\hat{\mathbf{\Theta}}$, $\mathbf{\Gamma} = \hat{\mathbf{C}}^{-1}$, and $\mathbf{m}$ is defined as

$$\mathbf{m} \triangleq \begin{bmatrix} \mathbf{1}^T\boldsymbol{l} - \mathbf{1}^T\bar{\mathbf{z}} - \mathbf{1}^T\bar{\mathbf{K}}\bar{\mathbf{p}}_{-i} \\ \bar{\mathbf{R}}\mathbf{S}(\mathbf{\Omega}\boldsymbol{l} - \bar{\mathbf{\Psi}}\bar{\mathbf{K}}\bar{\mathbf{p}}_{-i} - \hat{\mathbf{\Theta}}\,\hat{\mathbf{z}}) \end{bmatrix}. \tag{5.17}$$

Finally, by obtaining $\hat{\mathbf{p}}_{-i}$ as a function of $\mathbf{v}_i$ from (5.12), and using the KKT conditions of RTM in (5.16), the sensitivity of $\delta$ with respect to $\mathbf{v}_i$ can be obtained:

$$\frac{\partial \delta}{\partial \mathbf{v}_i} = \frac{\partial \delta}{\partial \hat{\mathbf{p}}_{-i}} \cdot \frac{\partial \hat{\mathbf{p}}_{-i}}{\partial \mathbf{v}_i} = \frac{1}{\mathbf{1}^T \mathbf{e}} \frac{1}{\mathbf{1}^T \mathbf{h}} (\mathbf{1}^T \hat{\mathbf{K}} \mathbf{h} - \mathbf{r} \hat{\mathbf{K}} \mathbf{h}) \tag{5.18}$$

where $\mathbf{e}$ and $\mathbf{r}$ are defined in (5.8) and (5.9). Note that, the coefficient in (5.18) depends on the set of binding constraints in not only the RTM optimization problem in (5.4) but also the DAM optimization problem in (5.1). If a binding constraint becomes unbinding or an unbinding constraint becomes binding, then some or all vectors $\mathbf{e}$, $\mathbf{h}$, and $\mathbf{r}$ may change, but keeping the relationship between $\delta$ and $\mathbf{v}_i$ linear.

Since both $\lambda$ and $\delta$ are piecewise linear function of $\mathbf{v}_i$, their difference, i.e., $\boldsymbol{\Delta}_i$ is also a piecewise linear function of $\mathbf{v}_i$. The slope of such function is derived as in (5.6) by subtracting (5.18) from (5.14). This concludes the proof. ■

The above theorem explains how a CB may change the price difference between the DAM and RTM of the bus where it is placed. Given the sensitivity model for price gap in (5.6), can ISOs guarantee that a profitable CB helps the system efficiency by closing the price gap under different grid operational conditions? First, what ISOs expect from the sensitivity of the price gap needs to be understood. Recall from Section 5.1 that ISOs assume that increasing a supply (demand) CB at a bus decreases (increases) the DAM price and increases (decreases) the RTM price at that bus. In fact, ISOs believe that

$$\frac{\partial \boldsymbol{\Delta}_i}{\partial \mathbf{v}_i} = \frac{\partial \boldsymbol{\pi}_i}{\partial \mathbf{v}_i} - \frac{\partial \boldsymbol{\sigma}_i}{\partial \mathbf{v}_i} < 0 \tag{5.19}$$

Therefore, if $\boldsymbol{\Delta}_i > 0$, the market participants can earn profit by submitting supply CBs; on the other hand, from (5.19), the supply CBs close the price gap among DAM and RTM. The same argument can be done when $\boldsymbol{\Delta}_i < 0$ and the demand CBs are submitted. However, as we show in Section 5.3, this argument does not always hold in nodal electricity markets. In fact, the impact of a CB on the price gap of the bus where it is placed depends

Table 5.1: Generators Bids Parameters

| | | | Bids | | | | | |
|---|---|---|---|---|---|---|---|---|
| | | | $\alpha_1$ | $\beta_1$ | $\alpha_2$ | $\beta_2$ | $\alpha_3$ | $\beta_3$ |
| Scenario | 1 | DAM | 0.1 | 8 | - | - | 0.3 | 10 |
| | | RTM | 0.7 | 2 | 1.7 | 3 | 1.9 | 4 |
| | 2 | DAM | 0.1 | 8 | - | - | 0.3 | 10 |
| | | RTM | 0.7 | 2 | 1.7 | 3 | 1.9 | 4 |
| | 3 | DAM | 0.1 | 8 | - | - | 0.3 | 10 |
| | | RTM | 0.7 | 2 | 1.7 | 3 | **0.1** | **9** |

on the coefficients of the piece-wise linear functions in Theorem 1. Indeed, under each network operating condition; depending on the coefficients in (5.6); placing a CB may enforce convergence (desirable) or divergence (undesirable) of the DAM and RTM prices. Accordingly, compared to the impact of CBs in financial markets, the impact of CBs in nodal electricity markets is much more complicated. Unfortunately, it appears that the CB-related studies were not aware of such complex issues, and they could not address the concerns raised by ISOs on CBs performance, as we pointed out in Section 5.1.2.

## 5.3 Case Studies

In this section, we discuss a few illustrative examples to demonstrate the fundamental concepts that our proposed analysis can help explain. Consider the three-bus power network in Fig. 5.2(a). Generators $G_1$ and $G_3$ participate in both the DAM and RTM, while generator $G_2$ participates only in the RTM. All generators have quadratic cost functions in form of $0.5\alpha_i \mathbf{x}_i^2 + \beta_i \mathbf{x}_i$, and their values are shown in Table 5.1. The reactance for all transmission lines is 0.1 Ohm. The resistance is negligible. The load at bus 2 procures 75 MWh from the DAM. Its actual load is realized as 90 MWh at the RTM.

Three scenarios are studied under different grid conditions and transmission line capacities. The scenarios are as follow:

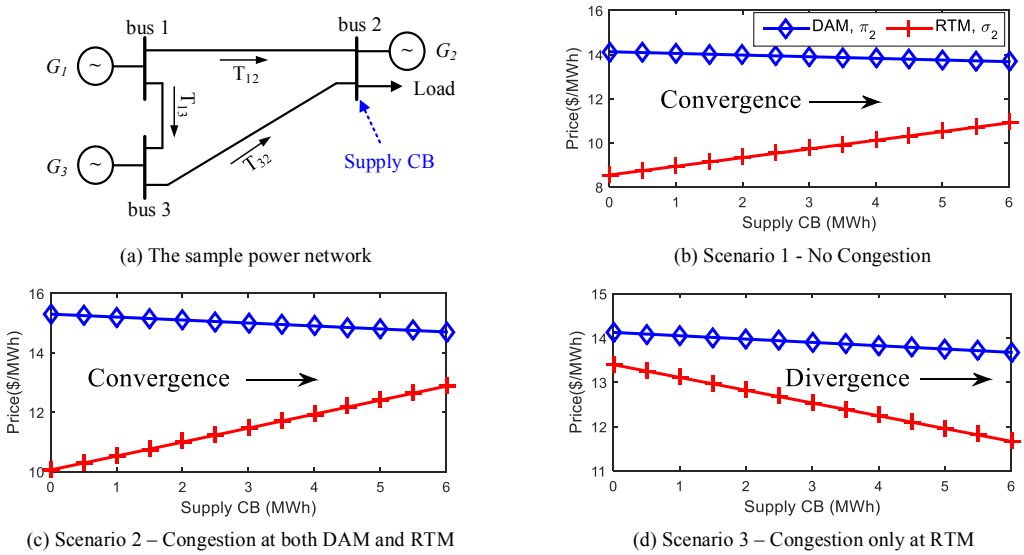


(a) The sample power network

(b) Scenario 1 - No Congestion

(c) Scenario 2 – Congestion at both DAM and RTM

(d) Scenario 3 – Congestion only at RTM

Figure 5.2: An example in a three-bus network to illustrate the intuitive (convergence) and counter-intuitive (divergence) results of convergence bidding.

**Scenario 1**: The transmission lines have sufficiently large capacity, such that no transmission line can be congested. If no CB is placed to the market, then the cleared market prices are $\boldsymbol{\pi}_1 = \boldsymbol{\pi}_2 = \boldsymbol{\pi}_3 = \$14.12$ and $\boldsymbol{\sigma}_1 = \boldsymbol{\sigma}_2 = \boldsymbol{\sigma}_3 = \$8.54$.

**Scenario 2**: The capacity of the transmission line between buses 1 and 3 ($T_{13}$) is 8 MW. All other parameters are the same as in Scenario 1. In this scenario, and in the absence of the CB, transmission line $T_{13}$ is congested at both DAM and RTM, as shown in Table 5.2. Accordingly, LMPs are different across different buses in both markets: $\boldsymbol{\pi}_1 = \$12.95$, $\boldsymbol{\pi}_2 = \$15.30$, $\boldsymbol{\pi}_3 = \$17.65$; and $\boldsymbol{\sigma}_1 = \$5.8$, $\boldsymbol{\sigma}_2 = \$10.05$, $\boldsymbol{\sigma}_3 = \$14.31$.

**Scenario 3**: The capacity of the transmission line between buses 1 and 2 ($T_{12}$) is 50 MW. The bid of $G_3$ submitted at the RTM is also changed as shown in Table 5.1. All other parameters are the same as in Scenario 1. In the absence of the CB, *no* transmission line is congested in the DAM, and we have: $\boldsymbol{\pi}_1 = \boldsymbol{\pi}_2 = \boldsymbol{\pi}_3 = \$14.12$; however, the transmission line between buses 1 and 2 *is* congested at the RTM, as shown in Table 5.2, note the bold underlined numbers. Therefore, we have: $\boldsymbol{\sigma}_1 = \$5.4$, $\boldsymbol{\sigma}_2 = \$13.4$, and $\boldsymbol{\sigma}_3 = \$9.4$.

Table 5.2: Line flows without CBs

| | | | Line flow (MW) | | |
|---|---|---|---|---|---|
| | | | $T_{12}$ | $T_{13}$ | $T_{32}$ |
| Scenario | 1 | DAM | 45.4 | 15.8 | 29.6 |
| | | RTM | 52.4 | 18.2 | 34.3 |
| | 2 | DAM | 41.5 | **8** | 33.5 |
| | | RTM | 46.9 | **8** | 38.9 |
| | 3 | DAM | 45.4 | 15.8 | 29.6 |
| | | RTM | **50.0** | 16.1 | 33.9 |

### 5.3.1 Numerical Results

In all scenarios, and in the absence of any CB, we have $\boldsymbol{\pi}_2 > \boldsymbol{\sigma}_2$, i.e., the DAM price is higher than the RTM price at bus 2. Therefore, placing a *supply* CB at bus 2 is *profitable* for the market participant. Of concern is whether or not such profitable supply CB can also help reducing the gap between the DAM and the RTM prices at bus 2, i.e., $\boldsymbol{\pi}_2 - \boldsymbol{\sigma}_2$.

The outcome of placing a supply CB at bus 2 and increasing its amount is shown in Fig. 5.2(b), (c), and (d) for Scenarios 1, 2, and 3, respectively. In Scenarios 1 and 2, placing a profitable supply CB at bus 2 results in price *convergence* at bus 2. However, under Scenario 3, placing a profitable supply CB at bus 2 results in price *divergence* at bus 2. This is *counter-intuitive* and against what ISOs expect from a CB [58].

### 5.3.2 Analytical Explanations

In this section, we use the analytical foundation that we developed in Theorem 1 to explain the numerical results that we observed earlier in the three scenarios.

**Scenario 1**: Since in this scenario, neither DAM nor RTM experience congestion, we have $\bar{\mathbf{D}} = \bar{\mathbf{R}} = \mathbf{0}$. From this, together with definition of $\mathbf{X}$ and $\mathbf{Y}$, we have $\mathbf{X} = \mathbf{Y} = \mathbf{0}$. By substituting these terms in (5.7), (5.8), and (5.9), we have:

$$\frac{\partial \boldsymbol{\Delta}_i}{\partial \mathbf{v}_i} = -\frac{1}{\mathbf{1}^T \boldsymbol{\Lambda} \mathbf{1}} \frac{1}{\mathbf{1}^T \boldsymbol{\Gamma} \mathbf{1}} (\mathbf{1}^T \boldsymbol{\Gamma} \mathbf{1} + \mathbf{1}^T \hat{\mathbf{K}} \boldsymbol{\Lambda} \mathbf{1}) < 0 \tag{5.20}$$

where the inequality is due to $\mathbf{\Lambda}$ and $\mathbf{\Gamma}$ being diagonal positive semi-definite matrices and $\hat{\mathbf{K}}$ comprising basis vectors. In fact, if the grid is not congested, then the electricity market reduces to a typical two-settlement financial market, in which CBs always improve market efficiency by reducing the price gap. In other words, what the ISOs often assume when they work with CBs is true for a nodal electricity market without transmission line congestion. For instance, in Scenario 1, we have $\mathbf{\Delta}_2 = 5.59 > 0$, and $\partial\mathbf{\Delta}_2/\partial\mathbf{v}_2 = -0.47 < 0$, which results in price convergence between DAM and RTM, as shown in Fig. 5.2(b).

**Scenario 2**: In this scenario, the congested transmission line at both DAM and RTM is $T_{13}$; therefore, $\bar{\mathbf{R}} = \bar{\mathbf{D}}$. Also, all marginal, i.e., price-maker, bids in the DAM are of type physical supply; i.e. $\hat{\mathbf{K}} = \mathbf{I}$ and $\hat{\mathbf{\Psi}} = \hat{\mathbf{\Phi}}_{-i}$. Thus, we have

$$\begin{aligned}\mathbf{r}\hat{\mathbf{K}}\mathbf{h} = \mathbf{r}\mathbf{h} = \mathbf{1}^T\mathbf{\Gamma}\mathbf{Y}(\mathbf{Y}\mathbf{\Gamma}\mathbf{Y}^T)^{-1} \\ \times (\mathbf{X}\mathbf{\Lambda}\mathbf{1} - \mathbf{X}\mathbf{\Lambda}\mathbf{X}^T(\mathbf{X}\mathbf{\Lambda}\mathbf{X}^T)^{-1}\mathbf{X}\mathbf{\Lambda}\mathbf{1}) = 0.\end{aligned} \tag{5.21}$$

Also, we can prove that $\mathbf{1}^T\mathbf{h}$ is always greater than zero:

$$\mathbf{1}^T\mathbf{h} = \|\mathbf{\Lambda}^{0.5}\mathbf{1} - \mathbf{\Lambda}^{0.5}\mathbf{X}^T(\mathbf{X}\mathbf{\Lambda}\mathbf{X}^T)^{-1}\mathbf{X}\mathbf{\Lambda}\mathbf{1}\|_2^2 > 0 \tag{5.22}$$

And similarly, $\mathbf{1}^T\mathbf{e} > 0$. Therefore, the sensitivity of the price gap to the supply CB is less than zero as expressed in (5.23):

$$\frac{\partial\mathbf{\Delta}_i}{\partial\mathbf{v}_i} = -\frac{\mathbf{1}^T\mathbf{h} + \mathbf{1}^T\mathbf{e}}{(\mathbf{1}^T\mathbf{h})(\mathbf{1}^T\mathbf{e})} \leq 0 \tag{5.23}$$

The above inequality explains the desirable results in Scenario 2. In fact, the conditions of this scenario guarantees that the supply CB results in price convergence. In particular, in this scenario, we have $\mathbf{\Delta}_2 = 5.25 > 0$, and $\partial\mathbf{\Delta}_2/\partial\mathbf{v}_2 = -0.57 < 0$, which supports the outcome of the supply CB on the price gap as shown in Fig. 5.2(c).

**Scenario 3**: In this scenario, we have $\boldsymbol{\Delta}_2 = 0.73 > 0$. Also, from (5.6) in Theorem 1, $\partial \boldsymbol{\Delta}_2 / \partial \mathbf{v}_2 = 0.21 > 0$. This is in contrast to what ISOs expect from CBs as expressed in (5.19). In other words, despite the fact that submitting a supply CB at bus 2 is reasonable for an independent CB market participant, the outcome to the market is in form of price *divergence* and against what is considered desirable by an ISO.

In summary, from Scenario 1, 2 and 3, it can be concluded that whether or not a CB causes price convergence between DAM and RTM in a congested nodal electricity market, depends on the sensitivity of the price gap to the CB, which relies on the grid conditions and transmission line congestion configuration. Therefore, while CBs always act as intended and results in price convergence in other financial market or nodal electricity market without congestion, but they may not act as expected in a nodal electricity market with congestion.

## 5.4 Conclusion

This section was motivated by the current state of uncertainty and debate about the impact of CBs in nodal electricity markets, which have been recently reported by multiple ISOs. To address this open problem, in this section, a fundamental sensitivity analysis has been introduced to understand how a CB may affect the DAM and RTM prices in a transmission-constrained nodal electricity market. Based upon the proposed sensitivity model and intuitive case studies, it is shown that the transmission line congestion can influence the impact of convergence bidding in nodal electricity markets in a way that is possible to degrade market efficiency. Specifically, under certain conditions, placing a CB at a bus can result in divergence (not convergence) between the DAM and RTM prices in that bus, which is counter-intuitive and undesirable.

# Chapter 6

# Conclusions and Future Work

## Conclusions

This thesis lies at the interface of operations research, economics, and engineering, with focus on building an analytical foundation to study and enhance the bids in wholesale electricity market. Therefore, as a first step in this thesis, a comprehensive analysis on the real bidding data from California electricity market has been done. It is concluded that compared to the supply side, the demand side in the California market is currently highly non-elastic, leading to many undesirable consequences such as price spikes and market power.

To improve the demand side participation in the market, a new demand bidding framework has been proposed that recognizes the special characteristics of smart loads. The bids in this bidding framework are called extended-time demand bids. The new framework resolves the problems of accommodating smart loads in the electricity market such as market instability and lack of equilibrium. Moreover, the proposed bidding structure also increases the market competitiveness due to expanding the competition domain and increasing demand elasticity. Moreover, a novel strategy for large smart loads to procure their required energy in electricity market has been introduced. The proposed strategy is

general and can be applied to both basic and complex smart load types, where the latter includes the loads that are uninterruptible, have per-time-slot consumption limits, ramp constraints, or comprise several smaller smart subloads. To investigate the performance of our design, a highly detailed illustrative case study along with multiple case studies based on the California energy market data are presented. We showed that the proposed optimal economic bidding approach outperforms the existing models.

Finally, the performance of financial players bids known as Convergence Bids (CBs) have been studied. The main reason of introducing CBs in the market is to close the price gap between day-ahead and real-time markets; accordingly improve the market efficiency. However, recent reports from ISOs show a state of uncertainty and debate about the impact of CBs in nodal electricity markets. Accordingly, in this thesis, we built an analytical foundation to explain under what conditions placing a CB at a bus in a nodal electricity market can decrease (increase) market efficiency. Specifically, it is shown that transmission line congestion can highly influence the performance of CBs. In particular, under certain transmission line congestion configurations, placing a CB at a bus can result in divergence (instead of convergence) between the day-ahead and real-time prices, which is counter-intuitive and undesirable. The proposed analysis would be beneficial to ISOs to understand how it is possible to shape the price difference caused by CBs across the power system.

## Future Work

This thesis can be extended in several following directions:

- In this thesis, a comprehensive analysis on the real bidding data in California electricity market in one year has been done. One may do the same analysis on other wholesale electricity markets in the US to see whether the demand side participation in those markets is non-elastic or not.

- The proposed bidding mechanism in Chapter 3 can be extended to cover the uncertainty of the smart loads and accommodate it into the extended-time demand bid.
- Developing a more comprehensive bidding strategy model compared to the proposed model in Chapter 4, to consider risk metrics such as Value at Risk (VaR) and Conditional Value at Risk (CVaR).
- While we studied the impact of CBs on price convergence (divergence) on the same bus where the CB was placed in Chapter 5, one can similarly study the impact also on price convergence (divergence) at buses other than where CBs are placed.
- Similar to the analysis in Chapter 5, one may extend it to explain the collective impact of a group of several CBs that are placed at different locations on the price gap of all system buses.

# Bibliography


[1] M. Shahidehpour and M. Alomoush, *Restructured electrical power systems: Operation: Trading, and volatility.* CRC Press, 2001.

[2] D. Kirschen and G. Strbac, *Fundamentals of Power System Economics.* John Wiley & Sons, 2004.

[3] P. A. Fedora, "Development of new england power pool's proposed markets," in *Proc. of the IEEE Hawaii International Conference on Systems Sciences*, Maui, HI, 1999.

[4] P. K. Narayan and R. Smyth, "Electricity consumption, employment and real income in australia evidence from multivariate granger causality tests," *Energy Policy*, vol. 33, no. 9, pp. 1109–1116, 2005.

[5] B. S. Tehrani and J. L. D. Attias, "Historical and theoretical approach of europoean market: How does electricity investment decision evolve with historical context?" in *Proc. of the IEEE International Conference on the European Energy Market*, Stockholm, Sweden, May 2013.

[6] H. Singh, "The california electricity market: an assessment of the first year of operations," in *Proc. of the IEEE Power Engineering Society Summer Meeting*, Edmonton, Canada, Jul. 1999.

[7] J. Yu, S. Teng, and J. Mickey, "Evolution of ERCOT market," in *Proc. of the IEEE Transmission and Distribution Conference and Exhibition: Asia and Pacific*, Dalian, China, 2005.

[8] A. Ott, "PJM: a full service iso market evolution," in *Proc. of the IEEE Power Engineering Society Summer Meeting*, Edmonton, Canada, Jul. 1999.

[9] A. Sadeghi-Mobarakeh and H. Mohsenian-Rad, "Strategic selection of capacity and mileage bids in california iso performance-based regulation market," in *Proc. of IEEE PES General Meeting*, 2016, pp. 1–5.

[10] M. Ghamkhari, A. Sadeghi-Mobarakeh, and H. Mohsenian-Rad, "Strategic bidding for producers in nodal electricity markets: A convex relaxation approach," *IEEE Trans. on Power Systems*, vol. 32, no. 3, pp. 2324–2336, 2017.

[11] A. Sadeghi-Mobarakeh and H. Mohsenian-Rad, "Optimal bidding in performance-based regulation markets: An mpec analysis with system dynamics," *IEEE Trans. on Power Systems*, vol. 32, no. 2, pp. 1282–1292, 2017.

[12] S. Borenstein, J. Bushnell, C. R. Knittel, and C. Wolfram, "Inefficiencies and market power in financial arbitrage: a study of california's electricity markets," *J. of Industrial Economics*, vol. 56, no. 2, pp. 347–378, 2008.

[13] A. Shahsavari, A. Sadeghi-Mobarakeh, E. Stewart, and H. Mohsenian-Rad, "Distribution grid reliability analysis considering regulation down load resources via micro-pmu data," in *Proc. of IEEE Smart Grid Communications (SmartGridComm)*, 2016, pp. 472–477.

[14] A. Sadeghi Mobarakeh, A. Rajabi-Ghahnavieh, and H. Haghighat, "A bi-level approach for optimal contract pricing of independent dispatchable dg units in distribution networks," *International Transactions on Electrical Energy Systems*, vol. 26, no. 8, pp. 1685–1704, 2016.

[15] S. Shao, T. Zhang, M. Pipattanasomporn, and S. Rahman, "Impact of TOU rates on distribution load shapes in a smart grid with PHEV penetration," in *Proc. of IEEE PES Transmission and Distribution Conference and Exposition*, New Orleans, LA, 2010 Apr.

[16] G. Marks, E. Wilcox, D. Olsen, and S. Goli, "Opportunities for demand response in California agricultural irrigation: A scoping study," Technical Report, Lawrence Berkeley National Laboratory, Jan. 2013.

[17] B. Aksanli, J. Venkatesh, L. Zhang, and T. Rosing, "Utilizing green energy prediction to schedule mixed batch and service jobs in data centers," in *Proc. of ACM Workshop on Power-Aware Computing and Systems*, Cascais, Portugal, Oct. 2011.

[18] Z. Liu, I. Liu, S. Low, and A. Wierman, "Pricing data center demand response," in *Proc. of ACM Sigmetrics*, Austin, TX, 2014 Jun.

[19] M. Ghamkhari and H. Mohsenian-Rad, "Energy and performance management of green data centers: A profit maximization approach," *IEEE Trans. on Smart Grid*, vol. 4, no. 2, pp. 1017–1025, Jun. 2013.

[20] Z. Yu, L. Jia, M. C. Murphy-Hoye, A. Pratt, and L. Tong, "Modeling and stochastic control for home energy management," *IEEE Trans. on Smart Grid*, vol. 4, no. 4, pp. 2244–2255, Dec. 2013.

[21] A. S. Al-Sumaiti, M. H. Ahmed, and M. M. A. Salama, "Electric power components and systems," *Smart Home Activities: A Literature Review*, vol. 42, no. 3-4, pp. 294–305, Feb. 2014.

[22] Z. Zhu, J. Tang, S. Lambotharan, W. Chin, and Z. Fan, "An integer linear programming based optimization for home demand-side management in smart grid," in *Proc. of IEEE PES ISGT*, Washington, DC, Jan. 2012.

[23] S. Meyn, P. Barooah, A. Busic, and J. Ehren, "Ancillary service to the grid from deferrable loads: The case for intelligent pool pumps in Florida," in *Proc. of IEEE Conference on Decision and Control*, Florence, Italy, Dec. 2013.

[24] A. Gholian, H. Mohsenian-Rad, Y. Hua, and J. Qin, "Optimal industrial load control in smart grid: A case study for oil refineries," in *Proc. of IEEE PES General Meeting*, Vancouver, Canada, Jul. 2013.

[25] P. Yang, G. Tang, and A. Nehorai, "A game-theoretic approach for optimal time-of-use electricity pricing," *IEEE Trans. on Power Systems*, vol. 28, no. 2, pp. 884–892, May 2013.

[26] A. Isemonger, "The benefits and risks of virtual bidding in multi-settlement markets," *Electricity Journal*, vol. 19, no. 9, pp. 26–36, 2006.

[27] Draft Final Proposal for the Design of Convergence Bidding, Available online at: http://www.caiso.com/2429/24291016c12990.pdf.

[28] M. Celebi, A. Hajos, and P. Hanser, "Virtual bidding: the good, the bad and the ugly," *The Electricity J.*, vol. 23, no. 5, pp. 16–25, 2010.

[29] C. D. Wolfram, "Strategic bidding in a multi-unit auction: An empirical analysis of bids to supply electricity," National Bureau of Economic Research, Tech. Rep., 1997.

[30] M. Kohansal, A. Sadeghi-Mobarakeh, and y. Mohsenian-Rad, Hamed booktitle=Proc. of IEEE Smart Grid Communications (SmartGridComm), "A data-driven analysis of supply bids in caiso market: Price elasticity and impact of renewables."

[31] E. Mansur, *Pricing behavior in the initial summer of the restructured PJM wholesale electricity market.* University of California Energy Institute, Berkeley, CA, 2001.

[32] A. Sadeghi-Mobarakeh, M. Kohansal, E. E. Papalexakis, and H. Mohsenian-Rad, "Data mining based on random forest model to predict the california iso day-ahead market prices," in *Proc. of IEEE PES Innovative Smart Grid Technologies Conference (ISGT)*, 2017, pp. 1–5.

[33] S. Fan and R. J. Hyndman, "The price elasticity of electricity demand in south australia," *Energy Policy*, vol. 39, no. 6, pp. 3709–3719, 2011.

[34] A. A. Mohdzin, M. Moradi, A. Khairuddin, A. Naderipour, and A. H. Khavari, "Estimation of elasticity of electricity demand in iran: New empirical evidence using aggregate data," in *Proc. of Student Conference on Research and Development.* IEEE, 2015.

[35] H. Mohsenian-Rad, V. Wong, J. Jatskevich, R. Schober, and A. Leon-Garcia, "Autonomous demand side management based on game-theoretic energy consumption scheduling for the future smart grid," *IEEE Trans. on Smart Grid*, vol. 1, no. 3, pp. 320–331, Dec. 2010.

[36] H. Mohsenian-Rad and A. Leon-Garcia, "Optimal residential load control with price prediction in real-time electricity pricing environments," *IEEE Trans. on Smart Grid*, vol. 1, no. 2, pp. 120–133, 2010.

[37] M. Alizadeh, T. H. Chang, and A. Scaglione, "On modeling and marketing the demand flexibility of deferrable loads at the wholesale leve," in *Proc. of IEEE HICSS*, Grand Wailea, HI, 2013 Jan.

[38] M. C. Caramanis, E. Goldis, P. A. Ruiz, and A. Rudkevich, "Power market reform in the presence of flexible schedulable distributed loads. new bid rules, equilibrium and tractability issues," in *Proc. of Annual Allerton Conference on Communication, Control, and Computing*, Urbana, IL, Oct 2012.

[39] D. Materassi, M. Roozbehani, and M. A. Dahleh, "Equilibrium price distributions in energy markets with shiftable demand," in *Proc. of IEEE Conference on Decision and Control*, Maui, HI, Dec. 2012.

[40] M. C. Caramanis and J. M. Foster, "Coupling of day ahead and real-time power markets for energy and reserves incorporating local distribution network costs and congestion," in *Proc. of Annual Allerton Conference on Communication, Control, and Computing*, Urbana, IL, Sep 2010.

[41] C. O. Adika and L. Wang, "Demand-Side Bidding Strategy for Residential Energy Management in a Smart Grid Environment," *IEEE Trans. on Smart Grid*, vol. 5, no. 4, pp. 1724–1733, Jul. 2014.

[42] M. C. Caramanis and J. M. Foster, "Uniform and complex bids for demand response and wind generation scheduling in multi-period linked transmission and distribution markets," in *Proc. of IEEE Conference on Decision and Control*, Orlando, FL, Dec. 2011.

[43] J. M. Foster and M. C. Caramanis, "Optimal power market participation of plug-in electric vehicles pooled by distribution feeder," *IEEE Trans. on Power Systems*, vol. 28, no. 3, pp. 2065–2076, Aug 2013.

[44] J. Saez-Gallego, M. Kohansal, A. Sadeghi-Mobarakeh, and J. M. Morales, "Optimal price-energy demand bids for aggregate price-responsive loads," *IEEE Trans. on Smart Grid*, 2017.

[45] H. Mohsenian-Rad, "Optimal demand bidding for time-shiftable loads," *IEEE Trans. on Power Systems*, vol. PP, no. 99, pp. 1–13, Jul. 2014.

[46] J. Medina, N. Muller, and I. Roytelman, "Demand Response and Distribution Grid Operations: Opportunities and Challenges," *IEEE Trans. on Smart Grid*, vol. 1, no. 2, pp. 193–198, Sep. 2010.

[47] H. Narimani and H. Mohsenian-Rad, "Autonomous demand response in heterogeneous smart grid topologies," in *Proc. of IEEE PES Conference on Innovative Smart Grid Technologies*, Washington, DC, Feb. 2013.

[48] M. Zarif, M. H. Javidi, and M. S. Ghazizadeh, "Self-Scheduling of Large Consumers With Second-Order Stochastic Dominance Constraints," *IEEE Trans. on Power Systems*, vol. 28, no. 1, pp. 289–299, Feb. 2013.

[49] H. Yan and H. Yan, "Optimal energy purchase in deregulated california energymarkets," in *Proc. of IEEE PES Winter Meeting*, Las Vegas, NV, 2000 Feb.

[50] J. Kambhu, "Trading risk, market liquidity, and convergence trading in the interest rate swap spread," *Economic Policy Review*, vol. 12, no. 1, 2006.

[51] P. Kondor, "Risk in dynamic arbitrage: the price effects of convergence trading," *The Journal of Finance*, vol. 64, no. 2, pp. 631–655, 2009.

[52] J. Liu and A. Timmermann, "Optimal convergence trade strategies," *Review of Financial Studies*, vol. 26, no. 4, pp. 1048–1086, 2013.

[53] S. Ledgerwood and J. Pfeifenberger, "Using virtual bids to manipulate the value of financial transmission rights," *The Electricity J.*, vol. 26, no. 9, pp. 9–25, 2013.

[54] G. K. Y. Shan, C. Prete and D. Miller, "Modeling and detecting bidding anomalies in day-ahead electricity markets."

[55] D. H. Choi and L. Xie, "Economic impact assessment of topology data attacks with virtual bids," *IEEE Transactions on Smart Grid*, vol. PP, no. 99, pp. 1–9, 2016.

[56] W. Tang, R. Rajagopal, K. Poolla, and P. Varaiya, "Model and data analysis of two-settlement electricity market with virtual bidding," in *55th IEEE Conference on Decision and Control (under review)*, 2016.

[57] 2015 annual report on market issues and performance, Available online at: http://www.caiso.com/Documents/2015AnnualReportonMarketIssuesandPerformance.pdf.

[58] "Virtual Transactions in the PJM Energy Markets", Available online at: http://www.pjm.com/~/media/documents/reports/20151012-virtual-bid-report.ashx.

[59] J. Parsons, C. Colbert, J. Larrieu, T. Martin, and E. Mastrangelo, "Financial arbitrage and efficient dispatch in wholesale electricity markets," *MIT Center for Energy and Environmental Policy Research*, 2015.

[60] M. Kohansal and H. Mohsenian-Rad, "A closer look at demand bids in california iso energy market," *IEEE Trans. on Power Systems*, vol. 31, no. 4, pp. 3330–3331, July 2016.

[61] California ISO Open Access Same-time Information System, Available online at: http://oasis.caiso.com.

[62] http://www.caiso.com/1c78/1c788230719c0.pdf.

[63] D. S. Kirschen, "Demand-side view of electricity markets," *IEEE Trans. on Power Systems*, vol. 18, no. 2, pp. 520–527, 2003.

[64] Business Practice Manuals of CAISO, Available online at: http://www.caiso.com/rules/Pages/BusinessPracticeManuals/Default.aspx.

[65] https://www.sdge.com/sites/default/files/regulatory/PUBLIC-SDGE-Bundled-Plan.pdf.

[66] Q. Zhou, W. Guan, and W. Sun, "Impact of demand response contracts on load forecasting in a smart grid environment," in *Proc. of IEEE Power and Energy Society General Meeting*, San Diego, CA, July 2012.

[67] M. Kohansal and H. Mohsenian-Rad, "Extended-time demand bids: A new bidding framework to accommodate time-shiftable loads," in *Proc. of the IEEE PES General Meeting*, Denver, CO, July 2015.

[68] F. Rahimi and A. Ipakchi, "Demand response as a market resource under the smart grid paradigm," *IEEE Trans. on Smart Grid*, vol. 1, no. 1, pp. 82–88, 2010.

[69] H. Akhavan-Hejazi, Z. Baharlouei, and H. Mohsenian-Rad, "Challenges and opportunities in large-scale deployment of automated energy consumption scheduling systems in smart grids," in *Proc of IEEE Conference on Smart Grid Communications*, Tainan City, Taiwan, 2012.

[70] F. Zhao, P. B. Luh, J. H. Yan, G. A. Stern, and S. C. Chang, "Bid cost minimization versus payment cost minimization: A game theoretic study of electricity auctions," *IEEE Trans. on Power Systems*, vol. 25, no. 1, pp. 181–194, Feb. 2010.

[71] M. Kohansal and H. Mohsenian-Rad, "Price-maker economic bidding in two-settlement pool-based markets: The case of time-shiftable loads," *IEEE Trans. on Power Systems*, vol. 31, no. 1, pp. 695–705, Jan. 2016.

[72] S. de la Torre, J. M. Arroyo, A. J. Conejo, and J. Contreras, "Price maker self-scheduling in a pool-based electricity market: A mixed-integer LP approach," *IEEE Trans. on Power Systems*, vol. 17, no. 4, pp. 1037–1042, Nov. 2002.

[73] California ISO, http://www.caiso.com/1c78/1c788230719c0.pdf.

[74] G. B. Sheblé, *Computational auction mechanisms for restructured power industry operation*. Norwell, MA: Kluwer Academic Publishers, 1999.

[75] G. Aneiros, J. M. Vilar, R. Cao, and A. M. S. Roque, "Functional prediction for the residual demand in electricity spot markets," *IEEE Trans. on Power Systems*, vol. 28, no. 2, pp. 4201–4208, Nov. 2013.

[76] M. Shahidehpour, H. Yamin, and Z. Li, *Market Operations in Electric Power Systems*. New York, NY: John Wiley & Sons, 2002.

[77] P. Kall and S. W. Wallace, *Stochastic Programing*, 2nd ed. John Wiley and Sons, 1994.

[78] K. Marti, *Stochastic Optimization Methods*. Springer, 2005.

[79] http://www.ibm.com/developerworks/downloads/ws/ilogcplex.

[80] http://www.mosek.com.

[81] S. Rao, *Engineering Optimization*, 4th ed. Hoboken, NJ: Wiley, 2009.

[82] W. Hogan, "Virtual bidding and electricity market design," *The Electricity Journal*, vol. 29, no. 5, pp. 33–47, 2016.

[83] A. Jha and F. A. Wolak, "Testing for market efficiency with transactions costs: An application to convergence bidding in wholesale electricity markets," in *Industrial Org. Seminar, Yale University*. Citeseer, 2013.

[84] I. Mercadal, "Dynamic competition and arbitrage in electricity markets: The role of financial players", Available online at: http://home.uchicago.edu/~ignaciamercadal/IgnaciaMercadalJMP.pdf.

[85] R. Li, A. Svoboda, and S. oren, "Efficiency impact of convergence bidding in the california electricity market," *Journal of Regulatory Economics*, vol. 48, no. 3, pp. 245–284, 2015.

[86] C. Woo, J. Zarnikau, E. Cutter, S. Ho, and H. Leung, "Virtual bidding, wind generation and california's day-ahead electricity forward premium," *The Electricity J.*, vol. 28, no. 1, pp. 29–48, 2015.

[87] S. Boyd and L. Vandenberghe, *Convex optimization*. Cambridge university press, 2004.